Finite Elements for the Stokes Problem

Daniele Boffi[1], Franco Brezzi[2], and Michel Fortin[3]

[1] Dipartimento di Matematica "F. Casorati", Università degli studi di Pavia, Via Ferrata 1, 27100 Pavia, Italy
daniele.boffi@unipv.it
[2] Istituto Universitario di Studi Superiori (IUSS) and I.M.A.T.I.–C.N.R., Via Ferrata 3, 27100 Pavia Pavia, Italy
brezzi@imati.cnr.it
[3] Département de Mathématiques et de Statistique, Pavillon Alexandre-Vachon, Université Laval, 1045, Avenue de la Mé decine, Quebec G1V 0A6, Canada
mfortin@mat.ulaval.ca

1 Introduction

Given a domain $\Omega \subset \mathbb{R}^n$, the Stokes problem models the motion of an incompressible fluid occupying Ω and can be written as the following system of variational equations,

$$\begin{cases} 2\mu \displaystyle\int_\Omega \underline{\underline{\varepsilon}}(\underline{u}) : \underline{\underline{\varepsilon}}(\underline{v})\, dx - \int_\Omega p \operatorname{div} \underline{v}\, dx = \int_\Omega \underline{f} \cdot \underline{v}\, dx, \quad \forall \underline{v} \in V, \\ \displaystyle\int_\Omega q \operatorname{div} \underline{u}\, dx = 0, \quad \forall q \in Q, \end{cases} \tag{1}$$

where $V = (H_0^1(\Omega))^n$ and Q is the subspace of $L^2(\Omega)$ consisting of functions with zero mean value on Ω. In this formulation $\underline{u}$ is the velocity of the fluid and p its pressure. A similar problem arises for the displacement of an incompressible elastic material.

An elastic material, indeed, can be modeled by the following variational equation, λ and μ being the Lamé coefficients

$$2\mu \int_\Omega \underline{\underline{\varepsilon}}(\underline{u}) : \underline{\underline{\varepsilon}}(\underline{v})\, dx + \lambda \int_\Omega \operatorname{div} \underline{u} \operatorname{div} \underline{v}\, dx = \int_\Omega \underline{f} \cdot \underline{v}\, dx, \quad \forall v \in V. \tag{2}$$

The case where λ is large (or equivalently when $\nu = \lambda/2(\lambda + \mu)$ approaches $1/2$) can be considered as an approximation of (1) by a penalty method. The limiting case is exactly (1) up to the fact that $\underline{u}$ is a displacement instead of a velocity. Problems where λ is large are quite common and correspond to almost incompressible materials.

It is also worth recalling that, defining $A\underline{u} = \underline{\mathrm{div}}\,\underline{\underline{\varepsilon}}(\underline{u})$, that in 2D reads

$$A\underline{u} = \begin{cases} \dfrac{\partial^2 u_1}{\partial x_1^2} + \dfrac{1}{2}\dfrac{\partial}{\partial x_2}\left(\dfrac{\partial u_1}{\partial x_2} + \dfrac{\partial u_2}{\partial x_1}\right), \\ \dfrac{\partial^2 u_2}{\partial x_2^2} + \dfrac{1}{2}\dfrac{\partial}{\partial x_1}\left(\dfrac{\partial u_1}{\partial x_2} + \dfrac{\partial u_2}{\partial x_1}\right), \end{cases} \tag{3}$$

we have $2\mu A\underline{u} = \mu\triangle\underline{u} + \mu\,\underline{\mathrm{grad}}\,\mathrm{div}\,\underline{u}$. Problems (1) and (2) are then respectively equivalent to

$$\begin{cases} -2\mu A\underline{u} + \underline{\mathrm{grad}}\,p = \mu\triangle\underline{u} + \underline{\mathrm{grad}}\,p = \underline{f}, \\ \mathrm{div}\,\underline{u} = 0, \\ \underline{u}|_\Gamma = 0, \end{cases} \tag{4}$$

and

$$-2\mu A\underline{u} - \lambda\,\underline{\mathrm{grad}}\,\mathrm{div}\,\underline{u} = -\mu\triangle\underline{u} - (\lambda+\mu)\,\underline{\mathrm{grad}}\,\mathrm{div}\,\underline{u} = \underline{f}. \tag{5}$$

Remark 1.1. The problems described above are, of course, physically unrealistic, as they involve body forces and homogeneous Dirichlet boundary conditions. The aim of doing so is to avoid purely technical difficulties and implies no loss of generality. The results obtained will be valid, unless otherwise stated, for all acceptable boundary conditions.

To approximate the Stokes problem, two approaches follow quite naturally from the preceding considerations. *The first* one is to use system (1) and to discretize $\underline{u}$ and p by standard (or less standard) finite element spaces. *The second* one is to use formulation (2) with λ large as a penalty approximation to system (1).

It rapidly became clear that both these approaches could yield strange results. In particular, the first one often led to nonconvergence of the pressure and the second one to a *locking mechanism*, the numerical solution being uniformly zero, or unnaturally small for big λ.

For velocity–pressure approximations, empirical cures were found by [46], [45] and others. At about the same time some elements using discontinuous pressure fields were shown to work properly [31], [35] from the mathematical point of view.

For the penalty method, the cure was found in selective or reduced integration procedures. This consisted in evaluating terms like $\int_\Omega \mathrm{div}\,\underline{u}\,\mathrm{div}\,\underline{v}\,dx$ by quadrature formulas of low order. This *sometimes* led to good results.

It was finally stated [50], even if the result was implicit in earlier works [8], that the analysis underlying the two approaches must be the same. Penalty methods are often equivalent to some mixed methods. In such cases, the penalty method works if and only if the associated mixed method works [9].

2 The Stokes Problem as a Mixed Problem

2.1 Mixed Formulation

We shall describe in this section how the Stokes problem (1) can be analyzed in the general framework of mixed methods. Defining $V = (H_0^1(\Omega))^n$, $\tilde{Q} = L^2(\Omega)$, and

$$a(\underline{u},\underline{v}) = 2\mu \int_\Omega \underline{\underline{\varepsilon}}(\underline{u}) : \underline{\underline{\varepsilon}}(\underline{v})\, dx, \tag{6}$$

$$b(\underline{v}, q) = -\int_\Omega q \operatorname{div} \underline{v}\, dx, \tag{7}$$

problem (1) can clearly be written in the form: find $\underline{u} \in V$ and $p \in \tilde{Q}$ such that

$$\begin{cases} a(\underline{u},\underline{v}) + b(\underline{v}, p) = (\underline{f},\underline{v}), \quad \forall \underline{v} \in V, \\ b(\underline{u}, q) = 0, \quad \forall q \in \tilde{Q}, \end{cases} \tag{8}$$

which is a mixed problem. Indeed, it can be observed that p is the Lagrange multiplier associated with the incompressibility constraint.

Remark 2.1. It is apparent, from the definition (7) of $b(\cdot,\cdot)$ and from the boundary conditions of the functions in V, that p, if exists, is defined up to a constant. Therefore, we introduce the space

$$Q = L^2(\Omega)/\mathbb{R}, \tag{9}$$

where two elements q_1, $q_2 \in L^2(\Omega)$ are identified if their difference is constant. It is not difficult to show that Q is isomorphic to the subspace of $L^2(\Omega)$ consisting of functions with zero mean value on Ω.

With this choice, our problem reads: find $\underline{u} \in V$ and $p \in Q$ such that

$$\begin{cases} a(\underline{u},\underline{v}) + b(\underline{v}, p) = (\underline{f},\underline{v}), \quad \forall \underline{v} \in V, \\ b(\underline{u}, q) = 0, \quad \forall q \in Q. \end{cases} \tag{10}$$

Let us check that our problem is well-posed. With standard procedure, we can introduce the following operators

$$B = -\operatorname{div} : (H_0^1(\Omega))^n \to L^2(\Omega)/\mathbb{R} \tag{11}$$

and

$$B^t = \underline{\operatorname{grad}} : L^2(\Omega)/\mathbb{R} \to (H^{-1}(\Omega))^n. \tag{12}$$

It can be shown (see, e.g., [64]) that

$$\operatorname{Im} B = Q \cong \left\{ q \in L^2(\Omega) : \int_\Omega q\, dx = 0 \right\}, \tag{13}$$

hence the operator B has a continuous lifting, and the continuous inf–sup condition is fulfilled. We also notice that, with our definition of the space Q, the kernel $\ker B^t$ reduces to zero.

The bilinear form $a(\cdot,\cdot)$ is coercive on V (see [32, 64]), whence the ellipticity in the kernel also will follow (i.e., A is invertible on $\ker B$).

We state the well-posedness of problem (10) in the following theorem.

Theorem 2.1. *Let* $\underline{f}$ *be given in* $(H^{-1}(\Omega))^n$. *Then there exists a unique* $(\underline{u}, p) \in V \times Q$ *solution to problem* (10) *which satisfies*

$$||\underline{u}||_V + ||p||_Q \leq C||\underline{f}||_{H^{-1}}. \tag{14}$$

Now choosing an approximation $V_h \subset V$ and $Q_h \subset Q$ yields the discrete problem

$$\begin{cases} 2\mu \displaystyle\int_\Omega \underline{\underline{\varepsilon}}(\underline{u}_h) : \underline{\underline{\varepsilon}}(\underline{v}_h)\, dx - \int_\Omega p_h \operatorname{div} \underline{v}_h\, dx = \int_\Omega \underline{f} \cdot \underline{v}_h\, dx, \quad \forall \underline{v}_h \in V_h, \\ \displaystyle\int_\Omega q_h \operatorname{div} \underline{u}_h\, dx = 0, \quad \forall q_h \in Q_h. \end{cases} \tag{15}$$

The bilinear form $a(\cdot, \cdot)$ is coercive on V; hence, according to the general theory of mixed approximations, there is no problem for the *existence* of a solution $\{\underline{u}_h, p_h\}$ to problem (15), while we might have troubles with the *uniqueness* of p_h. We thus try to obtain estimates of the errors $||\underline{u} - \underline{u}_h||_V$ and $||p - p_h||_Q$.

First we observe that, in general, the discrete solution $\underline{u}_h$ *needs not be divergence-free*. Indeed, the bilinear form $b(\cdot, \cdot)$ defines a discrete divergence operator

$$B_h = -\operatorname{div}_h : V_h \to Q_h. \tag{16}$$

(It is convenient here to identify $Q = L^2(\Omega)/\mathbb{R}$ and $Q_h \subset Q$ with their dual spaces). In fact, we have

$$(\operatorname{div}_h \underline{u}_h, q_h)_Q = \int_\Omega q_h \operatorname{div} \underline{u}_h\, dx, \tag{17}$$

and, thus, $\operatorname{div}_h \underline{u}_h$ turns out to be the L^2-projection of $\operatorname{div} \underline{u}_h$ onto Q_h.

The discrete divergence operator coincides with the standard divergence operator if $\operatorname{div} V_h \subset Q_h$. Referring to the abstract setting, we see that obtaining error estimates requires a careful study of the properties of the operator $B_h = -\operatorname{div}_h$ and of its transpose that we denote by $\underline{\operatorname{grad}}_h$.

The first question is to characterize the kernel $\ker B_h^t = \ker(\underline{\operatorname{grad}}_h)$. It might happen that $\ker B_h^t$ contains nontrivial functions In these cases $\operatorname{Im} B_h = \operatorname{Im}(\operatorname{div}_h)$ will be *strictly smaller* than $Q_h = P_{Q_h}(\operatorname{Im} B)$; this may lead to pathologies. In particular, if we consider a modified problem, like the one that usually originates when dealing with nonhomogeneous boundary conditions, the strict inclusion $\operatorname{Im} B_h \subset Q_h$ may even imply troubles with the existence of the solution. This situations is made clearer with the following example.

Example 2.1. Let us consider problem (4) with *nonhomogeneous boundary conditions*, that is let $\underline{r}$ be such that

$$\underline{u}|_\Gamma = \underline{r}, \quad \int_\Gamma \underline{r} \cdot \underline{n}\, ds = 0, \tag{18}$$

It is classical to reduce this case to a problem with homogeneous boundary conditions by first introducing a function $\tilde{\underline{u}} \in (H^1(\Omega))^n$ such that $\tilde{\underline{u}}|_\Gamma = \underline{r}$. Setting $\underline{u} = \underline{u}_0 + \tilde{\underline{u}}$ with $\underline{u}_0 \in (H_0^1(\Omega))^n$ we have to solve

$$\begin{cases} -2\mu A\underline{u}_0 + \underline{\mathrm{grad}}\, p = \underline{f} + 2\mu A\underline{\tilde{u}} = \underline{\tilde{f}}, \\ \mathrm{div}\, \underline{u}_0 = -\mathrm{div}\, \underline{\tilde{u}} = g, \quad \underline{u}_0|_\Gamma = 0 \end{cases} \tag{19}$$

with A defined in (3). We thus find a problem with a constraint $B\underline{u}_0 = g$ where $g \neq 0$. It may happen that the associated discrete problem fails to have a solution, because $g_h = P_{Q_h} g$ does not necessarily belongs to $\mathrm{Im}\, B_h$, whenever $\ker B_h^t \not\subset \ker B^t$. Discretization where $\ker(\underline{\mathrm{grad}}_h)$ is nontrivial *can therefore lead to ill-posed problems* in particular for some nonhomogeneous boundary conditions. Examples of such conditions can be found in [56, 57]. In general, any method that relies on extra compatibility conditions is a source of trouble when applied to more complicated (nonlinear, time-dependent, etc.) problems.

Let us now turn our attention to the study of the error estimates. Since the bilinear form $a(\cdot,\cdot)$ is coercive on V, we only have to deal with the inf–sup condition. The following proposition will be the starting point for the analysis of any finite element approximation of (10).

Proposition 2.1. *Let* $(\underline{u}, p) \in V \times Q$ *be the solution of* (10) *and suppose the following inf–sup condition holds true (with* k_0 *independent of* h*)*

$$\inf_{q_h \in Q_h} \sup_{\underline{v}_h \in V_h} \frac{\int_\Omega q_h\, \mathrm{div}\, \underline{v}_h\, dx}{||q_h||_Q ||\underline{v}_h||_V} \geq k_h \geq k_0 > 0. \tag{20}$$

Then there exists a unique $(\underline{u}_h, p_h) \in V_h \times Q_h$ *solution to* (15) *and the following estimate holds*

$$||\underline{u} - \underline{u}_h||_V + ||p - p_h||_Q \leq C \inf_{\underline{v}_h \in V_h,\ q_h \in Q_h} \left\{ ||\underline{u} - \underline{v}_h||_V + ||p - q_h||_Q \right\}. \tag{21}$$

Remark 2.2. Actually, as it has been already observed, the existence of the discrete solution $(\underline{u}_h, p_h)$ (when the right-hand side in the second equation of (10) is zero) is not a consequence of the inf–sup condition (20). However, we should not forget about the possible situation presented in Example 2.1.

Remark 2.3. We shall also meet cases in which the constant k_h is not bounded below by k_0. We shall then try to know precisely how it depends on h and to see whether a lower-order convergence can be achieved. When $\ker(\underline{\mathrm{grad}}_h)$ is nontrivial, we are interested in a weaker form of (20)

$$\sup_{\underline{v}_h \in V_h} \frac{\int_\Omega q_h\, \mathrm{div}\, \underline{v}_h\, dx}{||\underline{v}_h||_V} \geq k_h \inf_{q \in \ker(\underline{\mathrm{grad}}_h)} ||q_h - q||_{L^2(\Omega)}, \tag{22}$$

and in the dependence of k_h in terms of h.

Several ways have also been proposed to get a more direct and intuitive evaluation of how a finite element scheme can approximate divergence-free functions. One of them is the *constraint ratio*, that we denote by C_r, and which is defined as

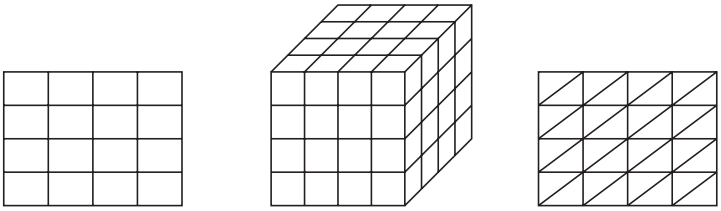

Fig. 1. Uniform meshes

$$C_r = \dim Q_h / \dim V_h. \tag{23}$$

It is, therefore, the ratio between the number of linearly independent constraints arising from the discrete divergence-free condition and the total number of degrees of freedom of the discrete velocity.

The value of C_r has no direct interpretation, *unless it is larger than* 1, which means that the number of constraints exceeds that of the variables. We then have a *locking phenomenon*.

Conversely, a small value of C_r implies a poor approximation of the divergence-free condition. It must however be emphasized that such a use of the constraint ratio has only a limited empirical value.

Another heuristic evaluation can be found by looking at the smallest representable vortex for a given mesh. This will be closely related to building a divergence-free basis (cf. Sect. 10). The idea behind this procedure [37] is that a discrete divergence-free function can be expressed as a sum of small vortices, that are, indeed, basis functions for $\ker B_h$. The size of the smallest vertices can be thought of as the equivalent of the smallest representable wavelenght in spectral methods.

In this context, we shall refer to a uniform mesh of n^2 rectangles, n^3 cubes or $2n^2$ triangles (Fig. 1). We must also quote the results of [67] who introduced a "patch test" to analyze similar problems. This patch test is only heuristic and does not yield a proof of stability. Moreover, such a test may be misleading in several cases.

3 Some Basic Examples

We start this section with some two-dimensional examples of possible choices for the spaces V_h and Q_h, namely the $P_1 - P_1$, $P_1 - P_0$ elements. These elements in general do not satisfy the inf–sup condition (20) and are not applicable in practice.

Then we present a complete analysis of the $P_2 - P_0$ element. Even though it might not be recommended to use this element because of its "unbalanced" approximation properties ($O(h^2)$ for V_h in the V-norm and only $O(h)$ for Q_h in the norm of Q), so that estimate (21) turns out to be suboptimal, the analysis of this element contains basic issues for getting familiar with the approximation of the Stokes problem. Moreover, the stability properties of this element will often be used as an intermediate step for the analysis of other, more efficient, elements.

Example 3.1. The $P_1 - P_1$ element

Let us consider a very simple case, that is, a P_1 continuous interpolation for both velocity and pressure, namely, using the notation of [24],

$$V_h = (\mathfrak{L}_1^1)^2 \cap V, \quad Q_h = \mathfrak{L}_1^1 \cap Q. \tag{24}$$

It is easy to check that if the number of triangles is large enough, then there exist nontrivial functions satisfying the *discrete* divergence-free condition. Thus no locking will occur and a solution can be computed. Indeed, this method would not provide an optimal approximation of the pressures by virtue of the unbalanced approximation properties of the discrete spaces (while Q_h achieves second order in L^2, V_h gives only first order in H^1). On the other hand, users of such methods (you can think of using also, for instance, (P_2-P_2), (Q_1-Q_1), etc.), soon became aware that their results were strongly mesh dependent. In particular, the computed pressures exhibited a very strange instability. This comes from the fact that for some meshes the kernel of the discrete gradient operator is nontrivial. This means that the solution obtained is determined only up to a given number of *spurious pressure modes*, [56, 57] and that, at best, some filtering will have to be done before accurate results are available. We shall come back later on to this phenomenon also named checkerboarding in Sect. 5. To better understand the nature of spurious pressure modes, the reader may check the results of Fig. 2 in which different symbols denote points where functions in $\ker(\underline{\mathrm{grad}}_h)$ must have equal values for a $(P_1 - P_1)$ approximation. In this case we have *three* spurious pressure modes. This also shows that there exists on this mesh one nontrivial discrete divergence-free function whereas a direct count would predict locking.

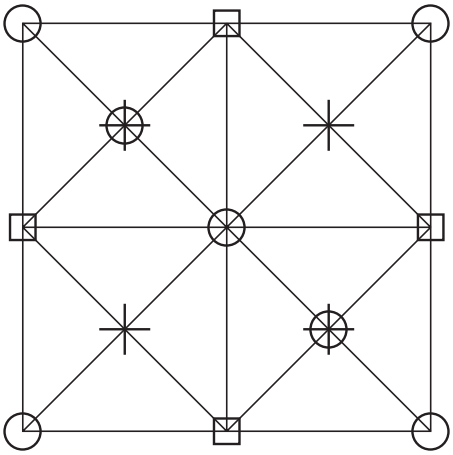

Fig. 2. Spurious pressure modes

Example 3.2. $P_1 - P_0$ *approximation*

This is probably the simplest element one can imagine for the approximation of an incompressible flow: one uses a standard P_1 approximation for the velocities and a piecewise constant approximation for the pressures. With the notation of [24] this would read

$$V_h = (\mathfrak{L}_1^1)^2 \cap V, \quad Q_h = \mathfrak{L}_0^0 \cap Q. \tag{25}$$

As the divergence of a P_1 velocity field is piecewise constant, this would lead to a divergence-free approximation. Moreover, this would give a well-balanced $O(h)$ approximation in estimate (21).

However, it is easy to see that such an element will not work for a general mesh. Indeed, consider a triangulation of a (simply connected) domain Ω and let us denote by

— t the number of triangles,
— v_I the number of internal vertices,
— v_B the number of boundary vertices.

We shall thus have $2v_I$ degrees of freedom (d.o.f.) for the space V_h (since the velocities vanish on the boundary) and $(t-1)$ d.o.f. for Q_h (because of the zero mean value of the pressures) leading to $(t-1)$ independent divergence-free constraints. By Euler's relations, we have

$$t = 2v_I + v_B - 2 \tag{26}$$

and thus

$$t - 1 > 2v_I \tag{27}$$

whenever $v_B > 3$. A function $\underline{u}_h \in V_h$ is thus overconstrained and a *locking phenomenon* is likely to occur: in general the only divergence-free discrete function is $\underline{u}_h \equiv 0$. When the mesh is built under certain restrictions, it is, however, possible that some linear constraints become dependent: this will be the case for the cross-grid macroelement (Fig. 3) which will be analyzed in Example 5.3.

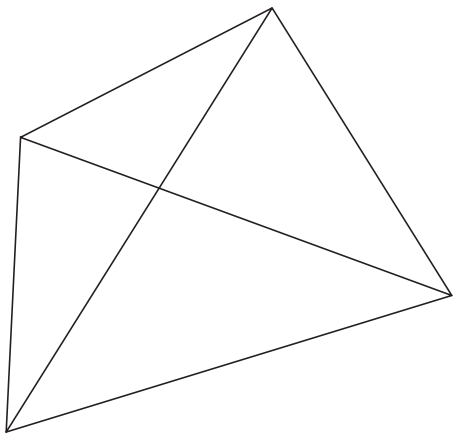

Fig. 3. The cross-grid element

Example 3.3. A stable approximation: the $P_2 - P_0$ element

Let us now move to the *stable* $P_2 - P_0$ element; namely, we use continuous piecewise quadratic vectors for the approximation of the velocities and piecewise constants for the pressures.

The discrete divergence-free condition can then be written as

$$\int_K \operatorname{div} \underline{u}_h \, dx = \int_{\partial K} \underline{u}_h \cdot \underline{n} \, ds = 0, \quad \forall K \in \mathcal{T}_h, \tag{28}$$

that is as a conservation of mass on every element. This is intuitively an approximation of $\operatorname{div} \underline{u}_h = 0$, directly related to the physical meaning of this condition. It is clear from error estimate (21) and standard approximation results that such an approximation will lead to the loss of one order of accuracy due to the poor approximation of the pressures. However, an augmented Lagrangian technique can be used, in order to recover a part of the accuracy loss (see Remark 3.2).

We are going to prove the following proposition.

Proposition 3.1. *The choice*

$$V_h = (\mathfrak{L}_2^1)^2 \cap V, \quad Q_h = \mathfrak{L}_0^0 \cap Q \tag{29}$$

fulfills the inf–sup condition (20)*.*

Proof. Before giving the rigorous proof of Proposition 3.1 we are going to sketch the main argument.

If we try to check the inf–sup condition by building a Fortin operator Π_h, then, given $\underline{u}$, we have to build $\underline{u}_h = \Pi_h \underline{u}$ such that

$$\int_\Omega \operatorname{div}(\underline{u} - \underline{u}_h) q_h \, dx = 0, \quad \forall q_h \in Q_h. \tag{30}$$

Since q_h is constant on every element $K \in \mathcal{T}_h$, this is equivalent to

$$\int_K \operatorname{div}(\underline{u} - \underline{u}_h) \, dx = \int_{\partial K} (\underline{u} - \underline{u}_h) \cdot \underline{n} \, ds = 0. \tag{31}$$

This last condition would be satisfied if $\underline{u}_h$ could be built in the following way. Let us denote by M_i and e_i, $i = 1, 2, 3$, the vertices and the sides of the triangular element K (Fig. 4); the midside nodes are denoted by M_{ij}. We then define

$$\underline{u}_h(M_i) = \underline{u}(M_i), \quad i = 1, 2, 3 \tag{32}$$

$$\int_{e_i} \underline{u}_h \, ds = \int_{e_i} \underline{u} \, ds. \tag{33}$$

Condition (33) can be fulfilled by a correct choice of $\underline{u}_h(M_{ij})$. Moreover this construction can be done at element level as the choice of $\underline{u}_h(M_{ij})$ is compatible on adjacent elements (that is, with this definition, $\underline{u}_h$ turns out to be continuous).

Although this is the basic idea, some technicalities must be introduced before a real construction is obtained. Indeed, for $\underline{u} \in (H_0^1(\Omega))^2$, condition (32) has no sense.

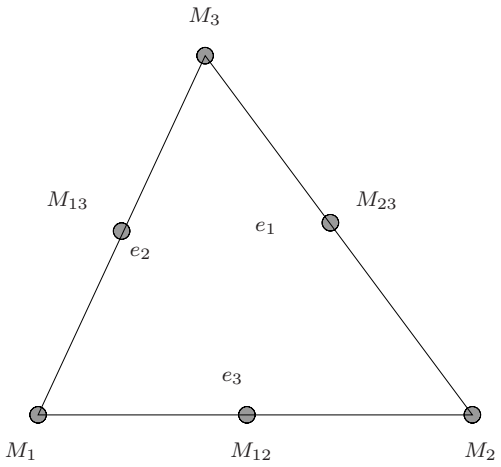

Fig. 4. Vertices, edges and midnodes

Let us then give a rigorous proof of Proposition 3.1. We denote by $\Pi_1 : V \to V_h$ the Clément interpolant [30]. We then have

$$\sum_K h_K^{2r-2} |\underline{v} - \Pi_1 \underline{v}|_{r,K}^2 \leq c ||\underline{v}||_{1,\Omega}^2, \quad r = 0, 1. \tag{34}$$

Setting $r = 1$ and using the triangular inequality $||\Pi_1 \underline{v}|| \leq ||\underline{v} - \Pi_1 \underline{v}|| + ||\underline{v}||$ gives

$$||\Pi_1 \underline{v}||_V \leq c_1 ||\underline{v}||_V, \quad \forall \underline{v} \in V. \tag{35}$$

We now modify Π_1 in a suitable way. Let us define $\Pi_2 : V \to V_h$ in the following way:

$$\Pi_2 \underline{v}|_K(M) = 0, \quad \forall M \text{ vertex of } K, \tag{36}$$

$$\int_e \Pi_2 \underline{u} \, ds = \int_e \underline{u} \, ds, \quad \forall e \text{ edge of } K. \tag{37}$$

By construction Π_2 satisfies

$$\int_\Omega \mathrm{div}(\underline{v} - \Pi_2 \underline{v}) q_h \, dx = 0, \quad \forall \underline{v}_h \in V_h, \; q_h \in Q_h \tag{38}$$

and a scaling argument gives

$$|\Pi_2 \underline{v}|_{1,K} = |\widehat{\Pi_2 \underline{v}}|_{1,\hat{K}} < c(K, \theta_0) ||\hat{\underline{v}}||_{1,\hat{K}} \leq c(K, \theta_0)(h_K^{-1} |\underline{v}|_{0,K} + |\underline{v}|_{1,K}). \tag{39}$$

We can now define

$$\Pi_h \underline{u} = \Pi_1 \underline{u} + \Pi_2(\underline{u} - \Pi_1 \underline{u}) \tag{40}$$

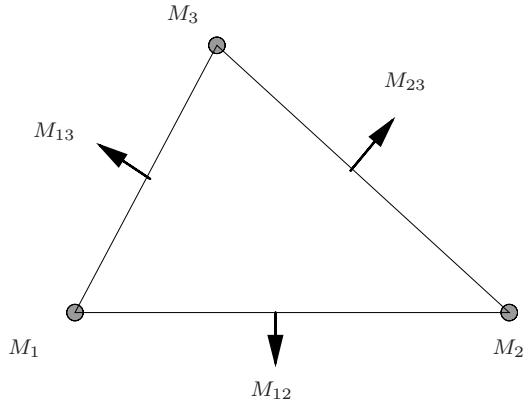

Fig. 5. Reduced $P_2 - P_0$ element

and observe that (39) and (34) imply

$$||\Pi_2(I - \Pi_1)\underline{u}||_V \leq c_2||\underline{u}||_V, \quad \forall \underline{v} \in V, \tag{41}$$

since

$$||\Pi_2(I - \Pi_1)\underline{v}||^2_{1,\Omega} = \sum_K ||\Pi_2(I - \Pi_1)\underline{v}||^2_{1,K} \tag{42}$$

$$\leq c \sum_K \left\{ h_K^{-2}||(I - \Pi_1)\underline{v}||^2_{0,K} + |(I - \Pi_1)\underline{v}|^2_{1,K} \right\} \leq c||\underline{v}||^2_{1,\Omega}. \tag{43}$$

Hence Π_h is a Fortin operator and the proof is concluded.

The above proof can easily be extended to more general cases. It applies to the $Q_2 - P_0$ quadrilateral element provided the usual regularity assumptions on quadrilateral meshes are made. A simple modification will hold for elements in which only the normal component of velocity is used as a d.o.f. at the midside nodes [37], [33], [11]. Indeed, if only the normal component of $\underline{u}_h$ is used as a degree of freedom, the $P_2 - P_0$ element becomes the element of Fig. 5 in which, on each side, the normal component of $\underline{u}_h$ is quadratic, whereas the tangential component is only linear. In this case we can define $\Pi_2\underline{v}$ by setting

$$\int_e (\Pi_2\underline{v} \cdot \underline{n})\, ds = \int_e \underline{v} \cdot \underline{n}\, ds \tag{44}$$

The above proof applies directly. The same remark is valid for the $Q_2 - P_0$ quadrilateral element.

Remark 3.1. The philosophical idea behind the $P_2 - P_0$ element is that we need one degree of freedom per each interface (actually, the normal component of the velocity) in order to control the jump of the pressures. This is basically the meaning

of the Green's formula (31). For three-dimensional elements, for instance, we would need some midface node instead of a midside node in order to control the normal flux from one element to the other.

In particular, we point out that adding *internal degrees of freedom* to the velocity space *cannot stabilize* elements with *piecewise constant pressures* which do not satisfy the inf–sup condition.

Remark 3.2. To reduce the loss of accuracy due to the unbalanced approximation properties of the spaces V_h and Q_h we can employ the augmented Lagrangian technique of [16]. The discrete scheme reads: find $(\underline{u}_h, p_h) \in V_h \times Q_h$ such that

$$\begin{aligned} &\int_\Omega \underline{\underline{\varepsilon}}(\underline{u}_h) : \underline{\underline{\varepsilon}}(\underline{v}_h)\, dx + h^{-1/2} \int_\Omega \operatorname{div} \underline{u}_h \operatorname{div} \underline{v}_h\, dx \\ &\qquad - \int_\Omega p_h \operatorname{div} \underline{v}_h\, dx = \int_\Omega \underline{f} \cdot \underline{v}_h\, dx \quad \forall \underline{v}_h \in V_h, \\ &\int_\Omega q_h \operatorname{div} \underline{u}_h\, dx = 0 \quad \forall q_h \in Q_h. \end{aligned} \tag{45}$$

Following [16] we have the following error estimate

$$||\underline{u} - \underline{u}_h||_V + ||p - p_h||_Q \le c h^{3/2} \inf_{\underline{v} \in V_h,\ q \in Q_h} \left(||\underline{u} - \underline{v}||_V + ||p - q||_Q \right). \tag{46}$$

4 Standard Techniques for Checking the Inf–Sup Condition

We consider in this section standard techniques for the proof of the inf–sup stability condition (20) that can be applied to a large class of elements. For ease of presentation, in this section we develop the theory only and postpone the examples to Sects. 6 and 7, for two- and three-dimensional schemes, respectively. However, after the description of each technique, we list some schemes for which that technique applies too.

Of course, the first method consists in the direct estimate of the inf–sup constant. In order to do that, we need to construct explicitly the operator $\underline{\operatorname{grad}}_h : Q_h \to V_h$ satisfying

$$\int_\Omega q_h \operatorname{div} \underline{\operatorname{grad}}_h\, q_h\, dx = ||q_h||_Q^2, \tag{47}$$

$$||\, \underline{\operatorname{grad}}_h\, q_h||_V \le c_h ||q_h||_Q, \tag{48}$$

for any $q_h \in Q_h$. If the constant c_h in (48) is bounded above, then the inf–sup condition (20) will hold true.

4.1 Fortin's Trick

An efficient way of proving the inf–sup condition (20) consists in using the technique presented in [36] which consists of building an interpolation operator Π_h as follows.

Proposition 4.1. *If there exists a linear operator $\Pi_h : V \to V_h$ such that*

$$\int_\Omega \operatorname{div}(\underline{u} - \Pi_h \underline{u}) q_h \, dx = 0, \quad \forall \underline{v} \in V,\ q_h \in Q_h, \tag{49}$$

$$||\Pi_h \underline{u}||_V \le c ||\underline{u}||_V. \tag{50}$$

then the inf–sup condition (20) *holds true.*

Remark 4.1. Condition (49) is equivalent to $\ker(\underline{\mathrm{grad}}_h) \subset \ker(\underline{\mathrm{grad}})$. An element with this property will present no spurious pressure modes.

In several cases the operator Π_h can be constructed in two steps as it has been done for the P_2–P_0 element in Proposition 3.1. In general it will be enough to build two operators $\Pi_1, \Pi_2 \in \mathcal{L}(V, V_h)$ such that

$$||\Pi_1 \underline{v}||_V \le c_1 ||\underline{v}||_V, \qquad \forall \underline{v} \in V, \tag{51}$$

$$||\Pi_2 (I - \Pi_1) \underline{v}||_V \le c_2 ||\underline{v}||_V, \quad \forall \underline{v} \in V, \tag{52}$$

$$\int_\Omega \operatorname{div}(\underline{v} - \Pi_2 \underline{v}) q_h = 0, \qquad \forall \underline{v} \in V,\ \forall q_h \in Q_h, \tag{53}$$

where the constants c_1 and c_2 are independent of h. Then the operator Π_h satisfying (49) and (50) will be found as

$$\Pi_h \underline{u} = \Pi_1 \underline{u} + \Pi_2 (\underline{u} - \Pi_1 \underline{u}). \tag{54}$$

In many cases, Π_1 will be the Clément operator of [30] defined in $H^1(\Omega)$.

On the contrary, the choice of Π_2 will vary from one case to the other, according to the choice of V_h and Q_h. However, the common feature of the various choices for Π_2 will be the following one: the operator Π_2 is constructed on each element K in order to satisfy (53). In many cases it will be such that

$$||\Pi_2 \underline{v}||_{1,K} \le c (h_K^{-1} ||\underline{v}||_{0,K} + |\underline{v}|_{1,K}). \tag{55}$$

We can summarize this results in the following proposition.

Proposition 4.2. *Let V_h be such that a "Clément's operator": $\Pi_1 : V \to V_h$ exists and satisfies* (34)*. If there exists an operator $\Pi_2 : V \to V_h$ such that* (53) *and* (55) *hold, then the operator Π_h defined by* (54) *satisfies* (49) *and* (50) *and therefore the discrete inf–sup condition* (20) *holds.*

Example 4.1. The construction of Fortin's operator has been used, for instance, for the sability proof of the $P_2 - P_0$ element (see Example 3.3).

4.2 Projection onto Constants

Following [19] we now consider a modified inf–sup condition.

$$\inf_{q_h \in Q_h} \sup_{\underline{v}_h \in V_h} \frac{\int_\Omega q_h \operatorname{div} \underline{v}_h \, dx}{||\underline{v}_h||_V ||q_h - \bar{q}_h||_Q} \ge k_0 > 0, \tag{56}$$

where $\bar{q}_h$ is the L^2-projection of q_h onto $\mathfrak{L}_0^0$ (that is, piecewise constant functions).

Proposition 4.3. *Let us suppose that the modified inf–sup condition* (56) *holds with k_0 independent of h. Assume moreover that V_h is such that, for any $q_h \in \mathfrak{L}_0^0 \cap Q$,*

$$\sup_{\underline{v}_h \in V_h} \frac{\int_\Omega q_h \operatorname{div} \underline{v}_h \, dx}{||\underline{v}_h||_V} \geq \gamma_0 ||q_h||_Q, \tag{57}$$

with γ_0 independent of h. Then the inf–sup condition (20) *holds true.*

Proof. For any $q_h \in Q_h$ one has

$$\begin{aligned} \sup_{\underline{v}_h \in V_h} \frac{b(\underline{v}_h, q_h)}{||\underline{v}_h||_V} &= \sup_{\underline{v}_h \in V_h} \left\{ \frac{b(\underline{v}_h, q_h - \bar{q}_h)}{||\underline{v}_h||_V} + \frac{b(\underline{v}_h, \bar{q}_h)}{||\underline{v}_h||_V} \right\} \\ &\geq \sup_{\underline{v}_h \in V_h} \frac{b(\underline{v}_h, \bar{q}_h)}{||\underline{v}_h||_V} - \sup_{\underline{v}_h \in V_h} \frac{b(\underline{v}_h, q_h - \bar{q}_h)}{||\underline{v}_h||_V} \\ &\geq \gamma_0 ||\bar{q}_h||_Q - ||q_h - \bar{q}_h||_0, \end{aligned} \tag{58}$$

which implies

$$\sup_{\underline{v}_h \in V_h} \frac{b(\underline{v}_h, q_h)}{||\underline{v}_h||_V} \geq \frac{k_0 \gamma_0}{1 + k_0} ||\bar{q}_h||_Q. \tag{59}$$

Putting together (56) and (59) proves the proposition.

Remark 4.2. In the case of *continous pressures* schemes, hypothesis (57) can be replaced with the following approximation assumption: for any $\underline{v} \in V$ there exists $\underline{v}^I \in V_h$ such that

$$||\underline{v} - \underline{v}^I||_{L^2(\Omega)} \leq c_1 h ||\underline{v}||_V, \quad ||\underline{v}^I||_V \leq c_2 ||\underline{v}||_V. \tag{60}$$

The details of the proof can be found in [19] when the mesh is quasiuniform. The quasiuniformity assumption is actually not needed, as it can be shown with an argument similar to the one which will be presented in the next subsection (see, in particular, Remark 4.3).

Example 4.2. The technique presented in this section will be used, for instance, for the stability proof of the generalized two-dimensional Hood–Taylor element (see Sect. 8.2 and Theorem 8.1).

4.3 Verfürth's Trick

Verfürth's trick [66] applies to *continuous pressures* approximations and is essentially based on two steps. The first step is quite general and can be summarized in the following lemma.

Lemma 4.1. *Let Ω be a bounded domain in $\mathbb{R}^N$ with Lipschitz continuous boundary. Let $V_h \subset (H_0^1(\Omega))^2 = V$ and $Q_h \subset H^1(\Omega)$ be closed subspaces. Assume that there exists a linear operator Π_h^0 from V into V_h and a constant c (independent of h) such that*

$$||\underline{v}_h - \Pi_h^0 \underline{v}||_r \leq c \sum_{K \in \mathcal{T}_h} \left(h_K^{2-2r} ||\underline{v}||_{1,K}^2 \right)^{1/2}, \quad \forall \underline{v} \in V,\ r = 0, 1. \tag{61}$$

Then there exist two positive constants c_1 and c_2 such that, for every $q_h \in Q_h$,

$$\sup_{\underline{v} \in V_h} \frac{\int_\Omega q_h \operatorname{div} \underline{v}_h \, dx}{||\underline{v}_h||_V} \geq c_1 ||q_h||_Q - c_2 \left(\sum_{K \in \mathcal{T}_h} h_K^2 ||\operatorname{\underline{grad}} q_h||_{0,K}^2 \right)^{1/2}. \tag{62}$$

Proof. Given $q_h \in Q_h$, let $\bar{\underline{v}} \in V$ be such that

$$\frac{\int_\Omega q_h \operatorname{div} \bar{\underline{v}} \, dx}{||\bar{\underline{v}}||_V ||q_h||_Q} \geq \beta > 0, \tag{63}$$

where β is the continuous inf–sup constant. Then,

$$\begin{aligned}
\sup_{\underline{v}_h \in V_h} \frac{\int_\Omega q_h \operatorname{div} \underline{v}_h \, dx}{||\underline{v}_h||_V} &\geq \frac{\int_\Omega q_h \operatorname{div} \Pi_h^0 \bar{\underline{v}} \, dx}{||\Pi_h^0 \bar{\underline{v}}||_V} \geq \frac{1}{2c} \frac{\int_\Omega q_h \operatorname{div} \Pi_h^0 \bar{\underline{v}} \, dx}{||\bar{\underline{v}}||_V} \\
&= \frac{1}{2c} \frac{\int_\Omega q_h \operatorname{div} \bar{\underline{v}} \, dx}{||\bar{\underline{v}}||_V} + \frac{1}{2c} \frac{\int_\Omega q_h \operatorname{div} (\Pi_h^0 \bar{\underline{v}} - \bar{\underline{v}}) \, dx}{||\bar{\underline{v}}||_V} \\
&\geq \frac{\beta}{4c} ||q_h||_Q - \frac{1}{2c} \frac{\int_\Omega \operatorname{\underline{grad}} q_h \cdot (\Pi_h^0 \bar{\underline{v}} - \bar{\underline{v}}) \, dx}{||\bar{\underline{v}}||_V} \\
&\geq \frac{\beta}{4c} ||q_h||_Q - \left(\frac{1}{2} \sum_{K \in \mathcal{T}_h} h_K^2 ||\operatorname{\underline{grad}} q_h||_{0,K}^2 \right)^{1/2}.
\end{aligned} \tag{64}$$

Remark 4.3. Indeed, via a scaling argument, it can be shown that the last term in the right-hand side of equation (62) is equivalent to $||q_h - \bar{q}_h||_0$, where $\bar{q}_h$ denotes, as in the previous subsection, the L^2-projection onto the piecewise constants.

We are now in the position of stating the main result of this subsection. Note that Verfürth's trick consists in proving a kind of inf–sup condition where the zero norm of q_h is substituted by $h|q_h|_1$.

Proposition 4.4. *Suppose the hypotheses of Lemma 4.1 hold true. Assume, moreover, that there exists a constant c_3 such that, for every $q_h \in Q_h$,*

$$\sup_{\underline{v}_h \in V_h} \frac{\int_\Omega q_h \operatorname{div} \underline{v}_h}{||\underline{v}_h||_V} \geq c_3 \left(\sum_{K \in \mathcal{T}_h} h_K^2 |q_h|_{1,K}^2 \right)^{1/2}. \tag{65}$$

Then the standard inf–sup condition (20) *holds true.*

Proof. Let us multiply (62) by c_3 and (65) by c_2 and sum up the two equations. We have

$$(c_3 + c_2) \sup_{\underline{v}_h \in V_h} \frac{\int_\Omega q_h \operatorname{div} \underline{v}_h \, dx}{||\underline{v}_h||_V} \geq c_1 c_3 ||q_h||_Q, \tag{66}$$

that is, the inf–sup condition (20).

Example 4.3. The Verfürth's trick has been designed for the stability analysis of the Hood–Taylor method. It will be used for this purpose in Sect. 8.2 (see Theorem 8.1).

4.4 Space and Domain Decomposition Techniques

Sometimes the spaces V_h and Q_h decomposes into the sum (direct or not) of subspaces for which it might be easier to prove an inf–sup condition. This is the case, for instance, when a *domain decomposition* technique is employed. Some of the results we are going to present, can be viewed as a particular case of the macroelement technique which will be introduced in Sect. 4.5.

The next result has been presented and proved in [41].

Proposition 4.5. *Suppose that Ω can be decomposed as the union of disjoint subdomains with Lipschitz continuous boundaries*

$$\Omega = \bigcup_{r=1}^{R} \Omega_r \tag{67}$$

and that such decomposition is compatible with the mesh in the sense that each element of the mesh is contained in one subdomain. We make use of the following notation:

$$\begin{aligned} &V_{0,r} = \{\underline{v} \in V_h : \underline{v} = 0 \text{ in } \Omega \setminus \Omega_r\}, \\ &Q_{0,r} = \{q \in Q_h : \int_{\Omega_r} q\,dx = 0\}, \\ &K = \{q \in Q : q|_{\Omega_r} \text{ is constant}, \ r = 1, \dots, R\}. \end{aligned} \tag{68}$$

Suppose, moreover, that the spaces $V_{0,r}$ and $Q_{0,r}$ satisfy the following inf–sup condition

$$\inf_{q_h \in Q_{0\cdot r}} \sup_{\underline{v}_h \in V_{0,r}} \frac{\int_{\Omega_r} q_h \operatorname{div} \underline{v}_h \, dx}{||q_h||_Q ||\underline{v}_h||_V} \geq k_r > 0, \tag{69}$$

with k_r independent of h ($r = 1, \dots, R$) and that the following inf–sup condition between V_h and K holds true

$$\inf_{q_h \in K} \sup_{\underline{v}_h \in V_h} \frac{\int_{\Omega} q_h \operatorname{div} \underline{v}_h \, dx}{||q_h||_Q ||\underline{v}_h||_V} \geq k_K > 0, \tag{70}$$

with k_K independent of h. Then the spaces V_h and Q_h satisfy the inf–sup condition (20).

Sometimes it is not possible (or it is not the best choice) to partition Ω into *disjoint* subdomains. Let us describe the case of two overlapping subdomains. The following proposition can be checked by a direct computation.

Proposition 4.6. *Let Ω be the union of two subdomains Ω_1 and Ω_2 with Lipschitz continuous boundaries. With the notation of the previous proposition, suppose that the spaces $V_{0,r}$ and $Q_{0,r}$ satisfy the inf–sup conditions*

$$\inf_{q_h \in Q_{0,r}} \sup_{\underline{v}_h \in V_{0,r}} \frac{\int_{\Omega_r} q_h \operatorname{div} \underline{v}_h \, dx}{||q_h||_Q ||\underline{v}_h||_V} \geq k_r > 0, \tag{71}$$

for $r = 1, 2$. Then the spaces V_h and Q_h satisfy the condition

$$\inf_{q_h \in Q_h} \sup_{\underline{v}_h \in V_h} \frac{\int_\Omega q_h \operatorname{div} \underline{v}_h \, dx}{||q_h - \overline{q}_h||_Q ||\underline{v}_h||_V} \geq \frac{1}{\sqrt{2}} \min(k_1, k_2), \tag{72}$$

where, as in Sect. 4.2, we have denoted by $\overline{q}_h$ the L^2 projection of q_h onto the space $\mathfrak{L}_0^0$.

Another useful technique for proving the inf–sup condition can be found in [54]. This result is quite general; in particular, the decomposition of the spaces V_h and Q_h does not rely on a decomposition of the domain Ω. In [54] the following proposition is stated for a two-subspaces decomposition, but it obviously extends to more general situations.

Proposition 4.7. *Let Q_1 and Q_2 be subspaces of Q_h such that*

$$Q_h = Q_1 + Q_2. \tag{73}$$

If V_1, V_2 are subspaces of V_h and α_1, α_2 positive constants such that

$$\inf_{q_h \in Q_i} \sup_{\underline{v}_h \in V_i} \frac{\int_\Omega q_h \operatorname{div} \underline{v}_h \, dx}{||q_h||_Q ||\underline{v}_h||_V} \geq \alpha_i, \quad i = 1, 2 \tag{74}$$

and β_1, β_2 are nonnegative constants such that

$$\begin{aligned} \left| \int_\Omega q_1 \operatorname{div} \underline{v}_2 \, dx \right| &\leq \beta_1 ||q_1||_Q ||\underline{v}_2||_V, \quad q_1 \in Q_1, \ \forall \underline{v}_2 \in V_2, \\ \left| \int_\Omega q_2 \operatorname{div} \underline{v}_1 \, dx \right| &\leq \beta_2 ||q_2||_Q ||\underline{v}_1||_V, \quad q_2 \in Q_2, \ \forall \underline{v}_1 \in V_1, \end{aligned} \tag{75}$$

with

$$\beta_1 \beta_2 < \alpha_1 \alpha_2, \tag{76}$$

then the inf–sup condition (20) *holds true with k_0 depending only on α_i, β_i, $i = 1, 2$.*

Remark 4.4. Condition (76) is trivially true, for instance, when $\beta_1 \beta_2 = 0$ and $\alpha_1 \alpha_2 > 0$.

Example 4.4. Most of the technique presented in this section can be seen as a particular case of the macroelement technique (see Sect. 4.5) Proposition 4.6 will be used in Theorem 8.1 for the stability proof of the Hood–Taylor scheme.

4.5 Macroelement Technique

In this section we present a technique introduced by Stenberg (see [59, 60, 62, 61, 63]) which, under suitable hypotheses, reduces the matter of checking the inf–sup condition (20) to an algebraic problem. We refer also to [18] for related results in a somewhat different setting.

The present technique is based on a decomposition of the triangulation $\mathcal{T}_h$ into disjoint macroelements, where we refer to a *macroelement* as an open polygon (resp., polyhedron in $\mathbb{R}^3$) which is the union of adjacent elements.

Let us introduce some notation.

A macroelement M is said to be *equivalent* to a reference macroelement $\hat{M}$ if there exists a mapping $F_M : \hat{M} \to M$ such that

1. F_M is continuous and invertible;
2. $F_M(\hat{M}) = M$;
3. If $\hat{M} = \cup \hat{K}_j$, where K_j, $j = 1, \ldots, m$ are the elements defining $\hat{M}$, then $K_j = F_M(\hat{K}_j)$, $j = 1, \ldots, m$, are the elements of M;
4. $F_M|_{\hat{K}_j} = F_{K_j} \circ F_{\hat{K}_j}^{-1}$, $j = 1, \ldots, m$, where F_K denotes the affine mapping from the reference element to a generic element K.

We denote by $\mathcal{E}_{\hat{M}}$ the equivalence class of $\hat{M}$. We now introduce the discrete spaces associated with V_h and Q_h on the generic macroelement M (n is the dimension of Ω).

$$\begin{aligned} V_{0,M} &= \left\{ \underline{v} \in (H_0^1(M))^n : \underline{v} = \underline{w}|_M \text{ with } \underline{w} \in V_h \right\}, \\ Q_{0,M} &= \left\{ p \in L^2(\Omega) : \int_M p \, dx = 0, \; p = q|_M \text{ with } q \in Q_h \right\}. \end{aligned} \tag{77}$$

We finally introduce a space which corresponds to the kernel of B_h^t on the macroelement M.

$$K_M = \left\{ p \in Q_{0,M} : \int_M p \operatorname{div} \underline{v} \, dx = 0, \; \forall \underline{v} \in V_{0,m} \right\}. \tag{78}$$

The *macroelements condition* reads

$$K_M = \{0\}, \tag{79}$$

that is, the analogous (at a macroelement level) of the necessary condition for the discrete Stokes problem to be well-posed that the kernel of B_h^t reduces to the zero function.

Proposition 4.8. *Suppose that each triangulation $\mathcal{T}_h$ can be decomposed into disjoint macroelements belonging to a* fixed *number (independent of h) of equivalence classes $\mathcal{E}_{\hat{M}_i}$, $i = 1, \ldots, n$. Suppose, moreover, that the pair $V_h - \mathfrak{L}_0^0/\mathbb{R}$ is a stable Stokes element, that is,*

$$\inf_{q_h \in \mathfrak{L}_0^0/\mathbb{R}} \sup_{\underline{v}_h \in V_h} \frac{\int_\Omega q_h \operatorname{div} \underline{v}_h \, dx}{||q_h||_Q ||\underline{v}_h||_V} \geq \beta > 0, \tag{80}$$

with β independent of h. Then the macroelement condition (79) *(for every $M \in \mathcal{E}_{\hat{M}_i}$, $i = 1, \ldots n$) implies the inf–sup condition* (20)*.*

Proof. We do not enter the technical details of the proof, for which we refer to [59]. The basic arguments of the proof are sketched in Remark 4.5.

Remark 4.5. The macroelement condition (79) is strictly related to the *patch test* commonly used in the engineering practice (cf., e.g., [67]). However, the count of the degrees of freedom is clearly insufficient by itself. Hence, let us point out how the hypotheses of Proposition 4.8 are important.

Hypothesis (79) (the macroelement condition) implies, via a compactness argument, that a discrete inf–sup condition holds true between the spaces $V_{0,M}$ and $Q_{0,M}$. The *finite* number of equivalent macroelements classes is sufficient to conclude that the corresponding inf–sup constants are uniformly bounded below by a positive number.

Then, we are basically in the situation of the domain decomposition technique of Sect. 4.4. We now use hypothesis (80) to control the constant functions on each macroelement and to conclude the proof.

Remark 4.6. Hypothesis (80) is satisfied in the two-dimensional case whenever V_h contains piecewise quadratic functions (see Sect. 3). In the three-dimensional case things are not so easy (to control the constants we need extra degrees of freedom on the faces, as observed in Remark 3.1. For this reason, let us state the following proposition which can be proved with the technique of Sect. 4.2 (see Remark 4.2) and which applies to the case of *continuous pressures* approximations.

Proposition 4.9. *Let us make the same assumptions as in Proposition 4.8 with* (80) *replaced by the condition of Remark 4.2 (see* (60)*). Then, provided* $Q_h \subset C^0(\Omega)$*, the inf–sup condition* (20) *holds true.*

Remark 4.7. The hypothesis that the macroelement partition of $\mathcal{T}_h$ is *disjoint* can be weakened, in the spirit of Proposition 4.6, by requiring that each element K of $\mathcal{T}_h$ belongs at most to a finite number N of macroelements with N independent of h.

Example 4.5. The macroelement technique can be used in order to prove the stability of several schemes. Among those, we recall the $Q_2 - P_1$ element (see Sect. 6.4) and the three-dimensional generalized Hood–Taylor scheme (see Theorem 8.2).

4.6 Making Use of the Internal Degrees of Freedom

This subsection presents a general framework providing a general tool for the analysis of finite element approximations to incompressible materials problems.

The basic idea has been used several times on particular cases, starting from [31] for discontinuous pressures and from [2] and [3] for continuous pressures. We are going to present it in its final general form given by [23]. It consists essentially in stabilizing an element by adding suitable bubble functions to the velocity field.

In order to do that, we first associate to every finite element discretization $Q_h \subset Q$ the space

$$B(\underline{\mathrm{grad}}\, Q_h) = \left\{ \underline{\beta} \in V : \underline{\beta}|_K = b_K \,\underline{\mathrm{grad}}\, q_h|_K \text{ for some } q_h \in Q_h \right\}, \tag{81}$$

where b_K is a bubble function defined in K. In particular, we can take as B_K the standard cubic bubble if K is a triangle, or a biquadratic bubble if K is a square or other

obvious generalizations in 3D. In other words, the restriction of a $\underline{\beta} \in B(\underline{\mathrm{grad}}\, Q_h)$ to an element K is the product of the bubble functions b_K times the gradient of a function of $Q_h|_K$.

Remark 4.8. Notice that the space $B(\underline{\mathrm{grad}}\, Q_h)$ is not defined through a basic space $\hat{B}$ on the reference element. This could be easily done in the case of *affine* elements, for all the reasonable choices of Q_h. However, this is clearly *unnecessary*: if we know how to compute q_h on K we also know how to compute $\underline{\mathrm{grad}}\, q_h$ and there is no need for a reference element.

We can now prove our basic results, concerning the two cases of continuous or discontinuous pressures.

Proposition 4.10. *(Stability of continuous pressure elements). Assume that there exists an operator $\Pi_1 \in \mathfrak{L}(V, V_h)$ satisfying the property of the Clément interpolant* (34)*. If $Q_h \subset C^0(\Omega)$ and V_h contains the space $B(\underline{\mathrm{grad}}\, Q_h)$ then the pair (V_h, Q_h) is a stable element, in the sense that it satisfies the inf–sup condition* (20)*.*

Proof. We shall build a Fortin operator, like in Proposition 4.2. We only need to construct the operator Π_2. We define $\Pi_2 : V \to B(\underline{\mathrm{grad}}\, Q_h)$, on each element, by requiring

$$\begin{aligned} &\Pi_2 \underline{v}|_K \in B(\underline{\mathrm{grad}}\, Q_h)|_K = b_{3,K}\, \underline{\mathrm{grad}}\, Q_h|_K, \\ &\int_K (\Pi_2 \underline{v} - \underline{v}) \cdot \underline{\mathrm{grad}}\, q_h \, dx = 0, \quad \forall q_h \in Q_h. \end{aligned} \tag{82}$$

Problem (82) has obviously a unique solution and Π_2 satisfies (53). Finally (55) follows by a scaling argument. Hence Proposition 4.2 gives the desired result.

Corollary 4.1. *Assume that $Q_h \subset Q$ is a space of continuous piecewise smooth functions. If V_h contains $(\mathfrak{L}^1_1)^2 \oplus B(\underline{\mathrm{grad}}\, Q_h)$ then the pair (V_h, Q_h) satisfies the inf–sup condition* (20)*.*

Proof. Since V_h contains piecewise linear functions, there exists a Clément interpolant Π_1 satisfying (34). Hence we can apply Proposition (4.10).

We now consider the case of discontinuous pressure elements.

Proposition 4.11. *(Stability of discontinuous pressure elements). Assume that there exists an operator $\tilde{\Pi}_1 \in \mathfrak{L}(V, V_h)$ satisfying*

$$\begin{aligned} &||\tilde{\Pi}_1 \underline{v}||_V \le c||\underline{v}||_V, \quad \forall \underline{v} \in V, \\ &\int_K \mathrm{div}(\underline{v} - \tilde{\Pi}_1 \underline{v})\, dx = 0, \quad \forall \underline{v} \in V \; \forall K \in \mathcal{T}_h. \end{aligned} \tag{83}$$

If V_h contains $B(\underline{\mathrm{grad}}\, Q_h)$ then the pair (V_h, Q_h) is a stable element, in the sense that it satisfies the inf–sup condition (20)*.*

Proof. We are going to use Proposition 4.10. We take $\tilde{\Pi}_1$ as operator Π_1. We are not defining Π_2 on the whole V, but only in the subspace

$$V^0 = \left\{ \underline{v} \in V : \int_K \operatorname{div} \underline{v}\, dx = 0, \quad \forall K \in \mathcal{T}_h \right\}. \tag{84}$$

This will be enough, since we need to apply Π_2 to the difference $\underline{v} - \tilde{\Pi}_1 \underline{v}$ which is in V^0 by (83).

For every $\underline{v} \in V^0$ we define $\Pi_2 \underline{v} \in B(\underline{\operatorname{grad}}\, Q_h)$ by requiring that, in each element K,

$$\begin{aligned} &\Pi_2 \underline{v}|_K \in B(\underline{\operatorname{grad}}\, Q_h)|_K = b_{3,K}\, \underline{\operatorname{grad}}\, Q_h|_K, \\ &\int_K \operatorname{div}(\Pi_2 \underline{v} - \underline{v}) q_h\, dx = 0, \quad \forall q_h \in Q_h|_K. \end{aligned} \tag{85}$$

Note that (85) is uniquely solvable, if $\underline{v} \in V^0$, since the divergence of a bubble function has always zero mean value (hence the number of nontrivial equations is equal to $\dim(Q_h|_K) - 1$, which is equal to the number of unknowns; the nonsingularity then follows easily). It is obvious that Π_2, as given by (85), will satisfy (53) for all $\underline{v} \in V^0$. We have to check that

$$\|\Pi_2 \underline{v}\|_1 \le c \|\underline{v}\|_V, \tag{86}$$

which actually follows by a scaling argument making use of the following bound

$$|\widehat{\Pi_2 \underline{v}}|_{0,\hat{K}} \le c(\theta_0) |\hat{\underline{v}}|_{1,\hat{K}}. \tag{87}$$

Corollary 4.2. *(Two-dimensional case). Assume that $Q_h \subset Q$ is a space of piecewise smooth functions. If V_h contains $(\mathfrak{L}^1_2)^2 \oplus B(\underline{\operatorname{grad}}\, Q_h)$ then the pair (V_h, Q_h) satisfies the inf–sup condition* (20).

Proof. The stability of the $P_2 - P_0$ element (see Sect. 3 implies the existence of $\tilde{\Pi}_1$ as in Proposition 4.11.

Propositions 4.10 and 4.11 are worth a few comments. They show that almost any element can be stabilized by using bubble functions. For continuous pressure elements this procedure is mainly useful in the case of triangular elements. For discontinuous pressure elements it is possible to stabilize elements which are already stable for piecewise constant pressure field. Examples of such a procedure can be found in [34]. Stability with respect to piecewise constant pressure implies that at least one degree of freedom on each side or face of the element is linked to the normal component of velocity (see [37] and Remark 3.1).

Example 4.6. The use of internal degrees of freedom can be used in the stability analysis of several methods. For instance, we use it for the analysis of the MINI element (see Sects. 6.1 and 7.1) in the case of continuous pressures and of the Crouzeix–Raviart element (see Remark 6.1 and Sect. 7.2) in the case of discontinuous pressures.

5 Spurious Pressure Modes

For a given choice of V_h and Q_h, the space S_h of spurious pressure modes is defined as follows

$$S_h = \ker B_h^t = \left\{ q_h \in Q_h : \int_\Omega q_h \operatorname{div} \underline{v}_h \, dx = 0 \; \forall \underline{v}_h \in V_h \right\}. \tag{88}$$

It is clear that a necessary condition for the validity of the inf–sup condition (20) is the absence of spurios modes, that is,

$$S_h = \{0\}. \tag{89}$$

In particular, if S_h is nontrivial then the solution p_h to the discrete Stokes problem (15) is not unique, namely $p_h + s_h$ is still a solution when $s_h \in S_h$.

We shall illustrate how this situation may occur with the following example.

Example 5.1. The $Q_1 - P_0$ element

Among quadrilateral element, the $Q_1 - P_0$ element is the first that comes to mind. It is defined as (see Fig. 6):

$$V_h = (\mathfrak{L}^1_{[1]})^2 \cap V, \qquad Q_h = \mathfrak{L}^0_0 \cap Q. \tag{90}$$

This element is strongly related, for rectangular meshes, to some finite difference methods [38]. Its first appearence in a finite elment context seems to be in [46].

However simple it may look, the $Q_1 - P_0$ element is one of the hardest elements to analyze and many questions are still open about its properties. This element does not satisfy the inf–sup condition: it strongly depends on the mesh. For a regular mesh the kernel of the discrete gradients is one-dimensional. More precisely, $\underline{\mathrm{grad}}_h \, q_h = 0$ implies that q_h is constant on the red and black cells if the mesh is viewed as a *checkerboard* (Fig. 7). This means that one singular value of the operator $B_h = \mathrm{div}_h$ is zero. Moreover, it has been checked by computation [49] that a large number of positive singular values converge to zero when h becomes small. In [48] indeed it has been proved that the second singular value is $O(h)$ and is not bounded below (see also [52]). The $Q_1 - P_0$ element has been the subject of a vast literature.

We shall now present a few more examples and distinguish between local and global spurious pressure modes.

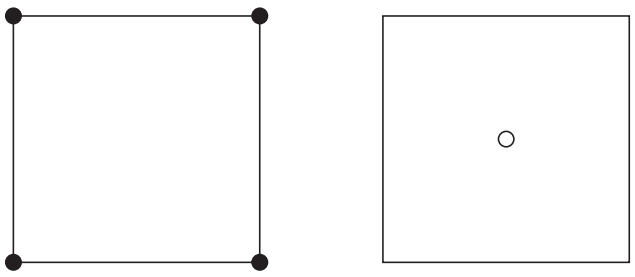

Fig. 6. The $Q_1 - P_0$ element

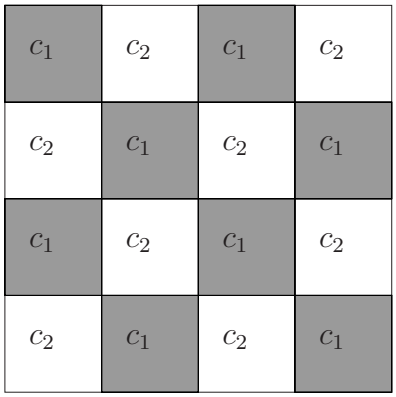

Fig. 7. Checkerboard spurious mode

Example 5.2. The crisscross $P_1 - P_0$ element

Let us consider a mesh of quadrilaterals divided into four triangles by their diagonals (Fig. 3). We observed in Example 3.2 that the $P_1 - P_0$ element, on *general meshes*, is affected by locking, that is, the computed velocity vanishes. On the mesh introduced above, however, it is easy to see that nonzero divergence-free functions can be obtained. The divergence is constant on each triangle. This means four linear relations between the values of the partial derivatives. It is easily seen that one of them can be expressed as a combination of the others, this fact being caused by equality of tangential derivatives along the diagonals. To make things simpler, we consider the case where the diagonals are orthogonal (Fig. 8) and we label by A, B, C, D the four triangles. We then have, by taking locally the coordinates axes along the diagonals, and denoting by u^K the restriction of a function of V_h to the element K,

$$\frac{\partial u_1^K}{\partial x_1} + \frac{\partial u_2^K}{\partial x_2} = 0, \quad K = A, B, C, D. \tag{91}$$

On the other hand, one has at the point M

$$\frac{\partial u_1^A}{\partial x_2} = \frac{\partial u_2^B}{\partial x_2}, \quad \frac{\partial u_1^A}{\partial x_1} = \frac{\partial u_1^C}{\partial x_1}, \quad \frac{\partial u_2^C}{\partial x_2} = \frac{\partial u_2^D}{\partial x_2}, \quad \frac{\partial u_1^B}{\partial x_1} = \frac{\partial u_1^D}{\partial x_1}. \tag{92}$$

It is easy to check that this makes one of the four conditions (91) redundant. The reader may check the general case by writing the divergence operator in a nonorthogonal coordinate system.

The consequence of the above discussion is that on each composite quadrilateral one of the four constant pressure values will be undetermined. The dimension of $\ker B_h^t$ will be *at least* as large as the number of quadrilaterals minus one.

Thus, three constraints remain on each composite quadrilateral element. If we admit that two of them can be controlled, using the methods of Sect. 4.6, by the "internal" node M, we obtain an element that is very similar to the $Q_1 - P_0$ element

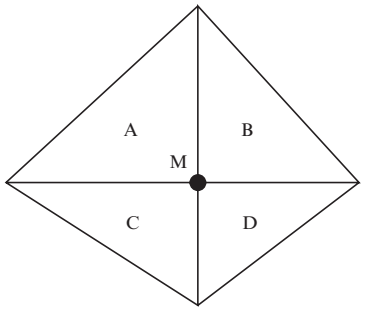

Fig. 8. The reference crisscross

with respect to the degrees of freedom. Indeed, it can be checked that on a regular mesh, an additional checkerboard mode occurs and that the behavior of this approximation is essentially the same as that of the $Q_1 - P_0$. These analogies have been pointed out, for instance, in [17].

The above example clearly shows the existence of two kinds of spurious pressure modes. Let us consider an element where S_h is nontrivial.

In the case of the crisscross $P_1 - P_0$ element presented in the previous example, $\dim S_h$ grows as h goes to 0 and there exists a basis of S_h with local support (that is, the support of each basis function can be restricted to one macroelement). We shall refer to these modes as *local spurious modes*. Such pressure modes can be eliminated by considering a composite mesh (in the previous example a mesh of quadrilaterals instead of triangles) and using a smaller space for the pressures by deleting some degrees of freedom from the composite elements.

If we now consider the $Q_1 - P_0$ example (see Example 5.1), the dimension of S_h does not grow when h goes to 0 and no basis can be found with a local support. We then have a *global spurious mode* which cannot be eliminated as easily as the local ones. Global modes usually appear on special (regular) meshes and are symptoms that the behavior of the element at hand is strongly mesh dependent and requires a special care. Some elements may generate both local and global modes as we have seen in the crisscross $P_1 - P_0$ method (see Example 5.2).

It must be emphasized that local spurious modes are source of troubles only when one prefers to work directly on the original mesh and not on the composite mesh on which they could easily be filtered out by a simple projection on each macroelement. We shall prove this in the next subsection in which a more precise framework will be given.

Example 5.3. The crisscross $P_2 - P_1$ element

Another simple example where a local mode occurs is the straightforward extension of the previous example to the case of a $P_2 - P_1$ approximation (Fig. 9). This means on each quadrilateral 12 discrete divergence-free constraints, and it is easily seen by the argument of Example 5.2, written at the point M, that one of them is

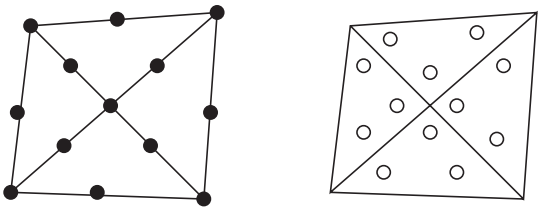

Fig. 9. The crisscross $P_2 - P_1$ element

redundant. Thus one spurious mode will appear for each composite quadrilateral. However, in this case, no global mode will appear. The analysis of this element is also related to the work of [29] by considering the stream function associated with a divergence-free function.

The presence of spurious modes can be interpreted as a signal that the pressure space used is in some sense too rich. We therefore can hope to find a cure by using a strict subspace $\hat{Q}_h$ of Q_h as the space of the discrete pressures, in order to obtain a stable approximation. The question arises whether or not this stability can be used to prove at least a partial result on the original approximation. One can effectively get some result in this direction.

6 Two-Dimensional Stable Elements

In this section we shall make use of the techniques presented in Sect. 4 to prove the stability for some of the most popular two-dimensional Stokes elements. The degrees of freedom corresponding to some of those are collected in Fig. 10.

We start with triangular elements and then we present schemes based on quadrilaterals.

The Hood–Taylor element (two- and three-dimensional) and its generalization will be presented in Sect. 8.

6.1 The MINI Element

This element, which is probably the cheapest one for the approximation of the Stokes equation, has been introduced in [3]. Given a mesh of triangles, the definition of the spaces is as follows

$$V_h = (\mathfrak{L}_1^1 \oplus B_3)^2 \cap V, \qquad Q_h = \mathfrak{L}_1^1 \cap Q, \tag{93}$$

where by B_3 we denotes the space of cubic bubbles.

The proof of the stability for the MINI element is an immediate consequence of Corollary 4.1

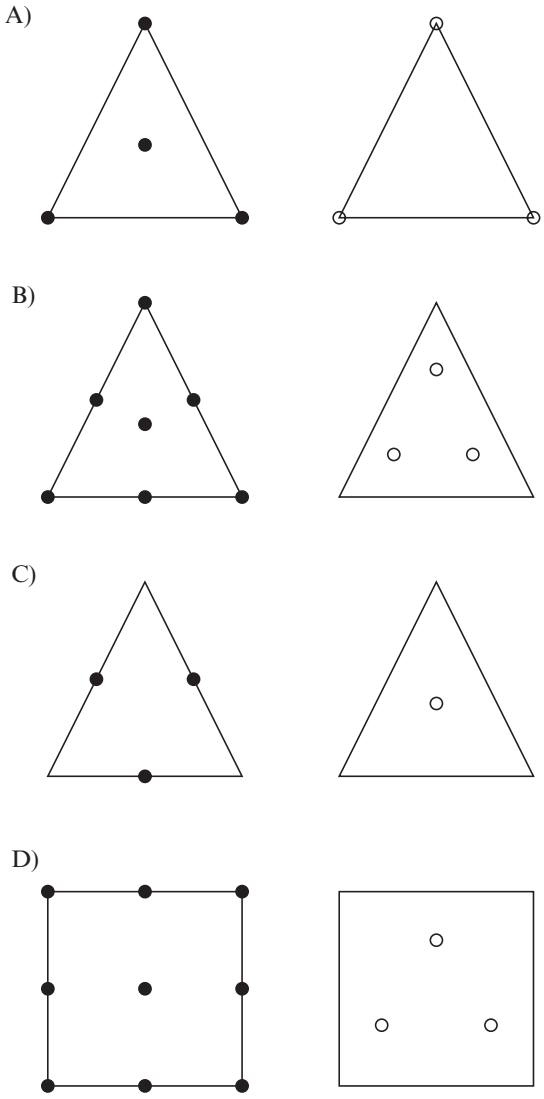

Fig. 10. Some stable two-dimensional Stokes elements: (a) the MINI element, (b) the Crouzeix–Raviart element, (c) the $P_1^{NC} - P_0$ element, (d) the $Q_2 - P_1$ element

6.2 The Crouzeix–Raviart Element

This element, presented in [31], is an enrichment to the $P_2 - P_0$ scheme which provides now well-balanced approximation properties. Given a mesh of triangles, the approximating spaces are

$$V_h = (\mathfrak{L}_2^1 \oplus B_3)^2 \cap V, \qquad Q_h = \mathfrak{L}_1^0 \cap Q. \tag{94}$$

The proof of the stability for this element can been carried out again with the help of Proposition 4.2. We use as operator Π_1 the Fortin operator of the $P_2 - P_0$ element (see also Proposition 4.11) and we take advantage of the internal degrees of freedom in V_h to define $\Pi_2 : V \to (B_3)^2$. Actually, we shall define $\Pi_2 \underline{v}$ only in the case when $\operatorname{div} \underline{v}$ has zero mean value in each K. This will be sufficient, since we shall use in practice $\Pi_2(\underline{v} - \Pi_1 \underline{v})$ and $\Pi_1 \underline{v}$ satisfies (83). For all K and for all $\underline{v}$ with

$$\int_K \operatorname{div} \underline{v} \, dx = 0, \tag{95}$$

we then set $\Pi_2 \underline{v}$ as the unique solution of

$$\Pi_2 \underline{v} \in (B_3(K))^2, \tag{96}$$

$$\int_K \operatorname{div}(\Pi_2 \underline{v} - \underline{v}) q_h \, dx = 0, \quad \forall q_h \in P_1(K). \tag{97}$$

Note that (96), (97) is a linear system of three equations $(\dim P_1(K) = 3)$ in two unknowns $(\dim(B_3(K))^2 = 2)$ which is compatible since $\underline{v}$ is assumed to satisfy (95) and, on the other hand, for every $\underline{b} \in (B_3(K))^2$ we clearly have

$$\int_K \operatorname{div} \underline{b} \, dx = 0. \tag{98}$$

We have only to prove that

$$||\Pi_2 \underline{v}||_{1,K} \leq c ||\underline{v}||_{1,K} \tag{99}$$

for all $\underline{v} \in V$ satisfying (95). Indeed (97) can be written as

$$\int_K (\Pi_2 \underline{v}) \cdot \underline{\operatorname{grad}} \, q_h \, dx = \int_K \operatorname{div} \underline{v} (q_h - \bar{q}_h) \, dx \tag{100}$$

where $\bar{q}_h$ is any piecewise constant approximation of q_h. A scaling argument yields

$$|\widehat{\Pi_2 \underline{v}}|_{0,\hat{K}} \leq c(\theta_0) |\hat{\underline{v}}|_{1,\hat{K}} \tag{101}$$

that easily implies (99).

Remark 6.1. We could prove the same result also as a consequence of Proposition 4.11. The same proof applies quite directly to the $Q_2 - P_1$ rectangular element (see Sect. 6.4). It can also be used to create nonstandard elements. For instance, in [34], bubble functions were added to a $Q_1 - P_0$ element in order to use a P_1 pressure field. This element is not more, but neither less, stable than the standard $Q_1 - P_0$ and gives better results in some cases.

6.3 $P_1^{NC} - P_0$ Approximation

We consider the classical stable nonconforming triangular element introduced in [31], in which midside nodes are used as degrees of freedom for the velocities. This generates a piecewise linear nonconforming approximation; pressures are

taken constant on each element (see Fig. 10). We do not present the stability analysis for this element, which does not fit within the framework of our general results, since V_h is not contained in V. However, we remark that this method is attractive for several reasons. In particular, the restriction to an element K of the solution $\underline{u}_h \in V_h$ is exactly divergence-free, since $\operatorname{div} V_h \subset Q_h$. Another important feature of this element is that it can be seen as a "mass conservation" scheme. The present element has been generalized to second order in [39]. It must also be said that coerciveness may be a problem for the $P_1^{NC} - P_0$ element, as it does not satisfy the discrete version of Korn's inequality. This issue has been deeply investigated and clearly illustrated in [5].

Remark 6.2. The generalization of nonconforming finite elements to quadrilaterals is not straightforward. In particular, approximation properties of the involved spaces are not obvious. More details can be found in [55].

6.4 $Q_k - P_{k-1}$ Elements

We now discuss the stability and convergence of a familiy of quadrilateral elements. The lowest order of this family, the $Q_2 - P_1$ element, is one of the most popular Stokes elements. Given $k \geq 2$, the discrete spaces are defined as follows:

$$V_h = (\mathfrak{L}^1_{[k]})^2 \cap V, \qquad Q_h = \mathfrak{L}^0_{[k-1]} \cap Q.$$

If the mesh is built of *rectangles*, the stability proof is an immediate consequence of Proposition 4.11, since (83) is satisfied for V_h (indeed, the $Q_2 - P_0$ is a stable Stokes element, see Remark 3.1). In the case of a general *quadrilateral* mesh things are not so easy; even the definition of the space Q_h is not so obvious and there have been different opinions, during the years, about two possible natural definitions. Following [15], we discuss in detail the case $k = 2$.

The $Q_2 - P_1$ Element

This element was apparently discovered around a blackboard at the Banff Conference on Finite Elements in Flow Problems (1979). Two different proofs of stability can be found in [41] and [59] for the rectangular case. This element is a relatively late comer in the field; the reason for this is that using a P_1 pressure on a quadrilateral is not a standard procedure. It appeared as a cure for the instability of the $Q_2 - Q_1$ element which appears quite naturally in the use of reduced integration penalty methods (see [9]). This last element is essentially related to the $Q_1 - P_0$ element and suffers the same problems altough to a lesser extent. Another cure can be obtained by adding internal nodes (see [34]).

On a general quadrilateral mesh, the space Q_h can be defined in two different ways: either Q_h consists of (discontinuous) piecewise linear functions, or it is built by considering three linear shape functions on the reference unit square and mapping them to the general elements like it is usually done for continuous finite elements. We point out that, since the mapping F_K from the reference element $\hat{K}$ to the general

element K in this case is bilinear but not affine, the two constructions are not equivalent. We shall refer to the first possibility as *unmapped* pressure approach and to the second one as *mapped* pressure approach.

In order to analyze the stability of either scheme, we use the macroelement technique presented in section 4.5 with macroelements consisting of one single element. We start with the case of the *unmapped* pressure approach; this is the original proof presented in [59]. Let M be a macroelement and $q_h = a_0 + a_x x + a_y y \in Q_{0,M}$ an arbitrary function in K_M. If $b(x, y)$ denote the biquadratic bubble function on K, then $\underline{v}_h = (a_x b(x, y), 0)$ is an element of $V_{0,M}$ and

$$0 = \int_M q_h \operatorname{div} \underline{v}_h \, dx \, dy = -\int_M \underline{\operatorname{grad}}\, q_h \cdot \underline{v}_h \, dx \, dy = -a_x \int_M b(x, y) \, dx \, dy$$

implies $a_x = 0$. In a similar way, we get $a_y = 0$ and, since the average of q_h on M vanishes, we have the macroelement condition $q_h = 0$.

We now move to the *mapped* pressure approach, following the proof presented in [15]. There, it is recalled that the macroelement condition (79) can be related to an algebraic problem in which we are led to proof that a 2×2 matrix is nonsingular. Actually, it turns out that the determinant of such matrix is a multiple of the Jacobian determinant of the function mapping the reference square $\hat{K}$ onto M, evaluated at the barycenter of $\hat{K}$. Since this number must be nonzero for any element of a well-defined mesh, we can deduce that the macroelement condition is satisfied in this case also, and then conclude that the stability holds thanks to Proposition 4.8.

So far, we have shown that either the *unmapped* and the *mapped* pressure approach gives rise to a stable $Q_2 - P_1$ scheme. However, as a consequence of the results proved in [6], we have that the mapped pressure approach *cannot achieve optimal approximation order*. Namely, the unmapped pressure space provides a second-order convergence in L^2, while the mapped one achieves only $O(h)$ in the same norm. In [15] several numerical experiments have been reported, showing that on general quadrilateral meshes (with constant distortion) the unmapped pressure approach provides a second-order convergence (for both velocity in H^1 and pressure in L^2), while the mapped approach is only suboptimally first-order convergent. It is interesting to remark that in this case also the convergence of the velocities is suboptimal, according to the error estimate (21).

7 Three-Dimensional Elements

Most elements presented in Sect. 6 have a three-dimensional extension. Some of them are schematically plotted in Fig. 11.

7.1 The MINI Element

Consider a regular sequence of decompositions of Ω into tetrahedra. The spaces are defined as follows:

$$V_h = (\mathfrak{L}_1^1 + B_4)^3 \cap V, \qquad Q_h = \mathfrak{L}_1^1 \cap Q,$$

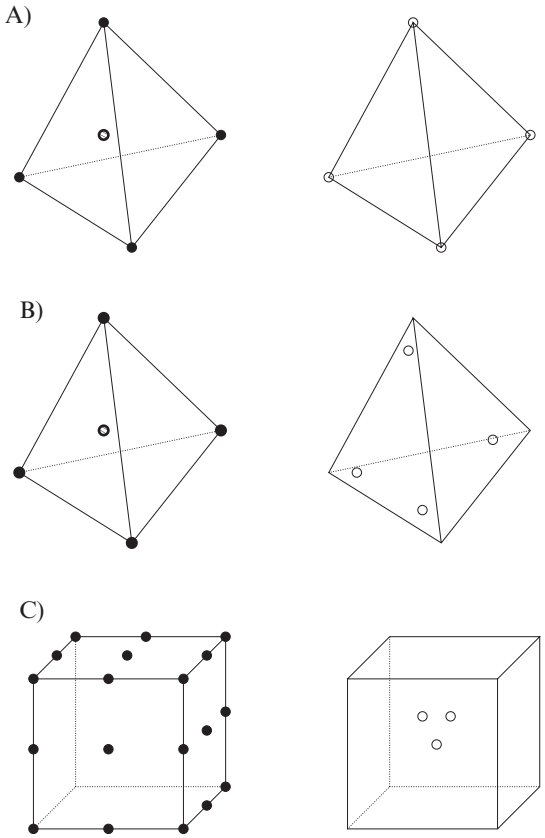

Fig. 11. Some stable three-dimensional Stokes elements: (a) the MINI element, (b) the Crouzeix–Raviart element, (c) the $Q_2 - P_1$ element

where B_4 denotes the space of quartic bubbles. Then the stability of this element follows easily, like in the 2D case, from Corollary 4.1.

7.2 The Crouseix–Raviart Element

The straightforward generalization of the Crouseix–Raviart element is given by

$$V_h = (\mathfrak{L}_1^1 + B_4)^3 \cap V, \qquad Q_h = \mathfrak{L}_1^0 \cap Q.$$

The stability is an easy consequence of Proposition 4.11.

7.3 $P_1^{NC} - P_0$ Approximation

The triangular $P_1^{NC} - P_0$ easily generalizes to tetrahedra in 3D. Also in this case, since $\operatorname{div} V_h \subset Q_h$, the restriction of the discrete solution to every element is truly divergence free.

7.4 $Q_k - P_{k-1}$ Elements

Given a mesh of hexahedrons, we define

$$V_h = (\mathfrak{L}^1_{[k]})^3 \cap V, \qquad Q_h = \mathfrak{L}^0_{[k-1]} \cap Q,$$

for $k \geq 2$. We refer to the two-dimensional case (see Sect. 6.4) for the definition of the pressure space. In particular, we recall that Q_h on each element consists of true polynomials and is not defined via the reference element. With the correct definition of the pressure space, the proof of stability for this element is a simple generalization of the corresponding two-dimensional version.

8 $P_k - P_{k-1}$ Schemes and Generalized Hood–Taylor Elements

The main result of this section (see Theorems 8.1 and 8.2) consists in showing that a family of popular Stokes elements satisfies the inf–sup condition (20). The first element of this family has been introduced in [45] and for this reason the members of the whole family are usually referred to as *generalized* Hood–Taylor elements.

This section is organized in two subsections. In the first one we discuss discontinuous pressure approximations for the $P_k - P_{k-1}$ element in the two-dimensional triangular case; it turns out that this choice is not stable in the lower-order cases and requires suitable conditions on the mesh sequences for the stability of the higher-order elements.

The last subsection deals with the generalized Hood–Taylor elements, which provide a continuous pressure approximation in the plane (triangles and quadrilaterals) and in the three-dimensional space (tetrahedrons and hexahedra).

8.1 $P_k - P_{k-1}$ Elements

In this subsection we shall recall the statement of a basic result by Scott and Vogelius [58] which, roughly speaking, says: under suitable assumptions on the decomposition $\mathfrak{T}_h$ (in triangles) the pair $V_h = (\mathfrak{L}^1_2)^2$, $Q_h = \mathfrak{L}^1_{k-1}$ satisfies the inf–sup condition for $k \geq 4$.

On the other hand, the problem of finding stable lower-order approximations has been studied by Qin [54], where interesting remarks are made on this scheme and where the possibility of filtering out the spurious pressure modes is considered.

In order to state in a precise way the restrictions that have to be made on the triangulation for higher-order approximations, we assume that Ω is a polygon, and that its boundary $\partial\Omega$ has no double points. In other words, there exists two continuous piecewise linear maps $x(t)$, $y(t)$ from $[0, 1[$ into $\mathbb{R}$ such that

$$\begin{cases} (x(t_1) = x(t_2) \text{ and } y(t_1) = y(t_2)) \text{ implies } t_1 = t_2, \\ \partial\Omega = \{(x, y) : x = x(t),\ y = y(t) \text{ for some } t \in [0, 1[\,\}. \end{cases} \tag{102}$$

Clearly, we will have $\lim_{t\to 1} x(t) = x(0)$ and $\lim_{t\to 1} y(t) = y(0)$. We remark that we are considering a less general case than the one treated by [58]. We shall make further restrictions in what follows, so that we are actually going to present a particular case of their results.

Let now V be a vertex of a triangulation $\mathfrak{T}_h$ of Ω and let $\theta_1, \ldots, \theta_p$, be the angles, at V, of all the triangles meeting at V, ordered, for instance, in the counterclockwise sense. If V is an internal vertex we also set $\theta_{p+1} := \theta_1$. Now we define $S(V)$ according to the following rules:

$$p = 1 \qquad \Rightarrow \qquad S(V) = 0 \tag{103}$$

$$p > 1,\ V \in \partial\Omega \qquad \Rightarrow \qquad S(V) = \max_{i=1,p-1} (\pi - \theta_1 - \theta_{i+1}) \tag{104}$$

$$V \notin \partial\Omega \qquad \Rightarrow \qquad S(V) = \max_{i=1,p} (\pi - \theta_i - \theta_{i+1}) \tag{105}$$

It is easy to check that $S(V) = 0$ if and only if all the edges of $\mathfrak{T}_h$ meeting at V fall on two straight lines. In this case V is said to be singular [58]. If $S(V)$ is positive but very small, then V will be "almost singular". Thus $S(V)$ measures how close V is to be singular.

We are now able to state the following result.

Proposition 8.1 ([58]). *Assume that there exists two positive constants c and δ such that*

$$ch \le h_K,\ \forall K \in \mathfrak{T}_h, \tag{106}$$

and

$$S(V) \ge \delta,\ \forall V \text{ vertex of } \mathfrak{T}_h. \tag{107}$$

Then the choice $V_h = (\mathfrak{L}^1_1)^2,\ Q_h = \mathfrak{L}^0_{k-1},\ k \le 4$, satisfies the inf–sup condition with a constant depending on c and δ but not on h.

Condition (107) is worth a few comments. The trouble is that $S(V) = 0$ makes the linear constraints on u_h, arising from the divergence-free condition, linearly dependent (see, also, Examples 5.2 and 5.3). When this linear dependence appears, some part of the pressure becomes unstable. In the present case, this unstable part could be filtered out.

Remark 8.1. The $P_k - P_{k-1}$ element can obviously be stabilized by adding bubbles to the velocity space in the spirit of Sect. 4.6 (see Proposition 4.11). For a less expensive stabilization, consisting in adding bubbles only in few elements, see [13].

8.2 Generalized Hood–Taylor Elements

In this subsection we recall the results proved in [12, 14] concerning the stability of the generalized Hood–Taylor schemes. On triangles or tetrahedra, velocities are approximated by a standard P_k element and pressures by a standard *continuous* P_{k-1}, that is $\underline{v}_h \in (\mathfrak{L}^1_k)^n$ $(n = 2, 3)$, $p \in \mathfrak{L}^1_{k-1}$. This choice has an analogue on rectangles or cubes using a Q_k element for velocities and a Q_{k-1} element for pressures. The

lowest order element (i.e., $k = 2$) has been introduced by Hood and Taylor [45]. Several papers are devoted to the analysis of this popular element. The degrees of freedom of some elements belonging to this family are reported in Fig. 12.

The first proof of convergence was given for the two-dimensional case in [10] where a weaker form of the inf–sup condition was used. The analysis was subsequently improved in [66] who showed that the classical inf–sup condition is indeed satisfied (see Verfürth's trick in Sect. 4.3). The macroelement technique can easily be used for the stability proof of the rectangular and cubic element (of any order) as well as of the tetrahedral case when $k = 2$ (see [59]). In [24] an alternative technique of proof has been presented for the triangular and tetrahedral cases when $k = 2$. This proof generalizes to the triangular case when $k = 3$ (see [21]). Finally, a general proof of convergence can be found in [12] and [14] for the triangular and tetrahedral case, respectively.

We now state and prove the theorem concerning the two-dimensional triangular case (see [12]).

Theorem 8.1. *Let Ω be a polygonal domain and $\mathcal{T}_h$ a regular sequence of triangular decompositions of it. Then the choice $V_h = (\mathfrak{L}^1_k \cap H^1_0(\Omega))^2$ and $Q_h = \mathfrak{L}^1_{k-1} \cap L^2_0(\Omega)$ satisfies the inf–sup condition* (20) *for any $k \geq 2$ if and only if each triangulation contains at least three triangles.*

Proof. **Step 1: Necessary part.** Let us show first that the hypothesis on the mesh is necessary. If $\mathcal{T}_h$ only contains one element, then it is easy to see that the inf–sup constant is zero (otherwise it should be $\operatorname{div} V_h \subset Q_h$, which is not the case since the functions in Q_h are not zero at the vertices). We shall show that if $\mathcal{T}_h$ contains only two triangles T_1 and T_2, then there exists one spurious pressure mode. This implies that also in this case the inf–sup constant vanishes. We choose the coordinate system (x, y) in such a way that the common edge of T_1 and T_2 lies on the y-axis. Moreover, we suppose that T_2 is the reference triangle and T_1 the symmetric one with respect to the x-axis, see Fig. 13. The general case can then be handled by means of suitable affine mappings.

We denote by $\lambda_{i,a}$ and $\lambda_{i,b}$ the barycentric coordinates relative to the vertices a and b, respectively, belonging to the element T_i, $i = 1, 2$. It is easy to check that it holds: $\lambda_{1,a} = 1 + x - y$, $\lambda_{1,b} = y$, $\lambda_{2,a} = 1 - x - y$, and $\lambda_{2,b} = y$. We shall also make use of the function $\lambda_{2,c} = x$. Let $L(x)$ be the Legendre polynomial of degree $k - 2$ on the unit interval with respect to the weight $w(x) = x(1 - x)^3$ and consider the function $p(x) \in Q_h$ defined as follows:

$$p'(x) = \begin{cases} -L(-x) & \text{for } x < 0, \\ L(x) & \text{for } x > 0. \end{cases} \tag{108}$$

We shall show that $\operatorname{grad} p$ is orthogonal to any velocity $\underline{v} \in V_h$. Since p does not depend on y, we can consider the first component v_1 of $\underline{v}$ only, which, by virtue of the continuity at $x = 0$ and of the boundary conditions, has the following general form:

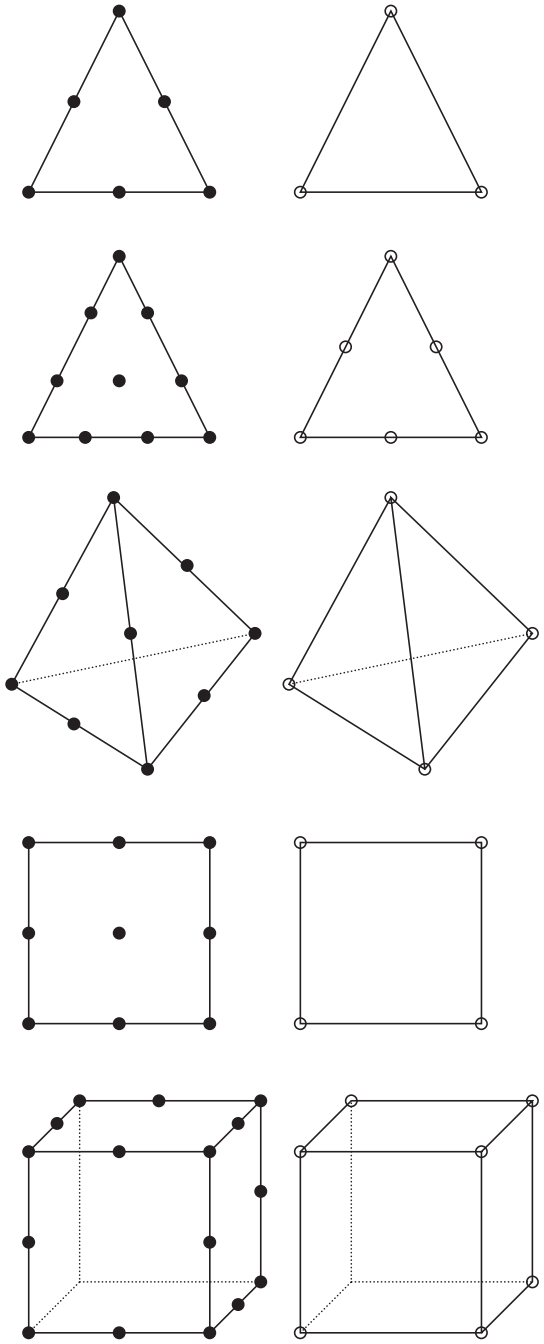

Fig. 12. Some stable elements belonging to the Hood–Taylor family

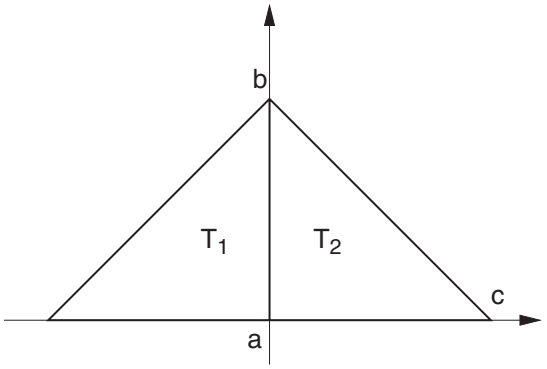

Fig. 13. The reference triangle and its symmetric

$$v_1 = \begin{cases} \lambda_{1,a}\lambda_{1,b}(C_{k-2}(y) + xA_{k-3}(x,y)) & \text{in } T_1, \\ \lambda_{2,a}\lambda_{2,b}(C_{k-2}(y) + xB_{k-3}(x,y)) & \text{in } T_2, \end{cases} \tag{109}$$

where the subscripts denote the degrees of the polynomials A, B and C. We then have

$$\begin{aligned} \int_{T_1\cup T_2} \underline{v}\cdot \operatorname{grad} p\, dx\, dy &= \int_{T_1} v_1 p'\, dx\, dy + \int_{T_2} v_1 p'\, dx\, dy \\ &= \int_{T_2} \lambda_{2,a}\lambda_{2,b} L(x) x (B_{k-3}(x,y) - A_{k-3}(-x,y))\, dx\, dy \\ &= \int_{T_2} \lambda_{2,a}\lambda_{2,b}\lambda_{2,c} L(x) q(x,y)\, dx\, dy \end{aligned} \tag{110}$$

where $q(x,y)$ is a polynomial of degree $k-3$ and where the term involving C disappears by virtue of the symmetries. The last integral reads

$$\int_{T_2} xy(1-x-y)L(x)q(x)\, dx\, dy = \int_0^1 xL(x)Q(x)\, dx \tag{111}$$

and an explicit calculation shows that $Q(x)$ is of the form

$$Q(x) = (1-x)^3 p_{k-3}(x), \tag{112}$$

where p_{k-3} is a polynomial of degree $k-3$. We can now conclude with the final computation

$$\int_{T_1\cup T_2} \underline{v}\cdot \operatorname{grad} p\, dx\, dy = \int_0^1 x(1-x)^3 L(x) p_{k-3}(x)\, dx = 0. \tag{113}$$

Step 2: Sufficient part. The idea of the proof consists in considering, for each h, a partition of the domain Ω in subdomains containing exactly three adjacent triangles.

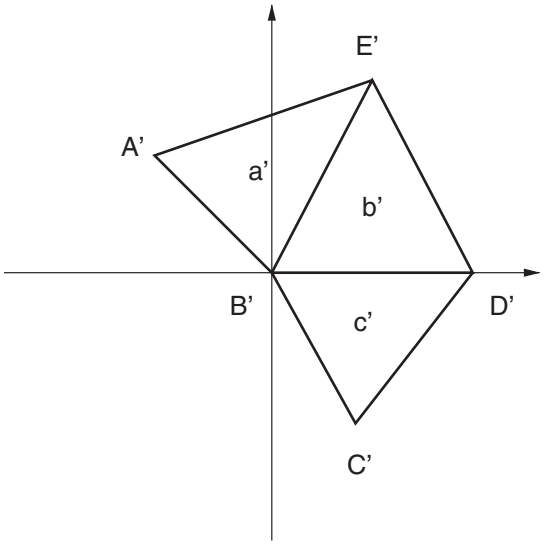

Fig. 14. A generic triplet of triangles

By making use of Proposition 4.6 and the technique presented in Sect. 4.2, it will be enough to prove the inf–sup condition for a single macroelement, provided we are able to bound the number of intersections between different subdomains (basically, everytimes two subdomains intersect each other, a factor $1/\sqrt{2}$ shows up in front of the final inf–sup constant). Indeed, it is possible to prove that, given a generic triangulation of a polygon, it can be presented as the disjoint union of triplets of triangles and of polygons that can be obtained as unions of triplets with at most three intersections.

Given a generic macroelement $a' \cup b' \cup c'$, consider the (x, y) coordinate system shown in Fig. 14, so that the vertices are $B' = (0, 0)$, $D' = (1, 0)$, $E' = (\alpha, \beta)$. By means of the affine mapping $x' = x + \alpha y$, $y' = \beta y$, the Jacobian of which is β, we can consider the macroelement $a \cup b \cup c$ shown in Fig. 15, so that b is the unit triangle. Since $\beta \neq 0$, the considered affine mapping is invertible. With an abuse in the notation, we shall now denote by Ω the triplet $a \cup b \cup c$ and by V_h and Q_h the finite element spaces built on it.

We denote by λ^a_{AB} the barycentric coordinate of the triangle a vanishing on the edge AB (analogous notation holds for the other cases). Moreover, we denote by $L^a_{i,x}(x)$ the i-th Legendre polynomial in $[x_A, 0]$, with respect to the measure $\mu_{a,x}$ defined by

$$\int_{x_A}^{0} f(x)\, d\mu_{a,x} = \int_a \lambda^a_{AB}\lambda^a_{AE} f(x)\, dx\, dy, \qquad \forall f(x) : [x_A, 0] \to \mathbb{R}, \tag{114}$$

where x_A is the x-coordinate of the vertex A. We shall make use of the following Legendre polynomials, which are defined in a similar way: $L^b_{i,x}$ (its definition involves λ^b_{ED} and λ^b_{BD}), $L^b_{i,y}$ (using λ^b_{BE} and λ^b_{BD}), and $L^c_{i,y}$ (using λ^c_{BC} and λ^c_{CD}).

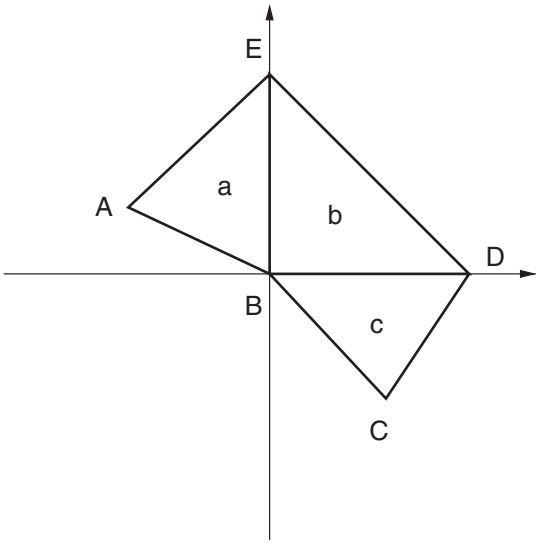

Fig. 15. A macroelement where b is the reference triangle

Standard properties of the Legendre polynomials ensures that we can normalize them, for instance, by requiring that they assume the same value (say 1) at the origin. We now prove by induction with respect to the degree k that a modified inf–sup condition holds true (see Verfürth's trick in Sect. 4.3). Namely, for any $q_h \in Q_h$, we shall construct $\underline{v}_h \in V_h$ such that

$$\begin{aligned} &-\int_{a\cup b\cup c} \underline{v}_h \cdot \operatorname{grad} q_h \, dx\, dy \geq c_1 ||\operatorname{grad} q_h||_0^2, \\ &||\underline{v}_h||_0 \leq c_2 ||\operatorname{grad} q_h||_0. \end{aligned} \tag{115}$$

The case $k = 2$. This is the original Hood–Taylor method. Given $p \in Q_h$, we define $\underline{v}_h = (v_1(x, y), v_2(x, y))$ triangle by triangle as follows:

$$v_1(x,y)|_a = -\lambda_{AB}^a \lambda_{AE}^a ||\operatorname{grad} p||_0 \cdot \sigma, \tag{116}$$

$$v_2(x,y)|_a = -\lambda_{AB}^a \lambda_{AE}^a \frac{\partial p}{\partial y}, \tag{117}$$

$$v_1(x,y)|_b = -\lambda_{ED}^b \lambda_{BD}^b ||\operatorname{grad} p||_0 \cdot \sigma - \lambda_{ED}^b \lambda_{EB}^b \frac{\partial p}{\partial x}, \tag{118}$$

$$v_2(x,y)|_b = -\lambda_{ED}^b \lambda_{BD}^b \frac{\partial p}{\partial y} - \lambda_{ED}^b \lambda_{EB}^b ||\operatorname{grad} p||_0 \cdot \tau, \tag{119}$$

$$v_1(x,y)|_c = -\lambda_{BC}^c \lambda_{CD}^c \frac{\partial p}{\partial x}, \tag{120}$$

$$v_2(x,y)|_c = -\lambda_{BC}^c \lambda_{CD}^c ||\operatorname{grad} p||_0 \cdot \tau, \tag{121}$$

where the quantities σ and τ are equal to ± 1 so that the expressions

$$H = \sigma || \operatorname{grad} p||_0 \left(\int_a \lambda^a_{AB} \lambda^a_{AE} \cdot \frac{\partial p}{\partial x} + \int_b \lambda^b_{ED} \lambda^b_{BD} \cdot \frac{\partial p}{\partial x} \right), \tag{122}$$

$$K = \tau || \operatorname{grad} p||_0 \left(\int_b \lambda^b_{EB} \lambda^b_{ED} \cdot \frac{\partial p}{\partial y} + \int_c \lambda^c_{BC} \lambda^c_{CD} \cdot \frac{\partial p}{\partial y} \right) \tag{123}$$

are nonnegative. First of all, we observe that $\underline{v}_h$ is an element of V_h: its degree is at most two in each triangle, it vanishes on the boundary and it is continuous across the the internal edges because so is the tangential derivative of p.

It easy to check that $||\underline{v}_h||_0 \leq c_1 || \operatorname{grad} p||_0$. In order to prove the first equation in (115), we shall show that the quantity $||| \operatorname{grad} p||| := -\int_\Omega \underline{v}_h \cdot \operatorname{grad} p$ vanishes only when $\operatorname{grad} p$ is zero. From the equality

$$\begin{aligned} 0 = ||| \operatorname{grad} p||| = & \int_a \lambda^a_{AB} \lambda^a_{AE} \left(\frac{\partial p}{\partial y} \right)^2 + H \\ & + \int_b \left(\lambda^b_{ED} \lambda^b_{EB} \left(\frac{\partial p}{\partial x} \right)^2 + \lambda^b_{ED} \lambda^b_{BD} \left(\frac{\partial p}{\partial y} \right)^2 \right) \\ & + K + \int_c \lambda^c_{BC} \lambda^c_{CD} \left(\frac{\partial p}{\partial x} \right)^2 \end{aligned} \tag{124}$$

it follows that

$$\frac{\partial p}{\partial y} = 0 \quad \text{in } a, \tag{125}$$

$$\frac{\partial p}{\partial x} = \frac{\partial p}{\partial y} = 0 \quad \text{in } b, \tag{126}$$

$$\frac{\partial p}{\partial x} = 0 \quad \text{in } c, \tag{127}$$

$$H = K = 0. \tag{128}$$

These last equations, together with the fact that each component of $\operatorname{grad} p$ is constant if $p \in Q_h$, easily imply that

$$\operatorname{grad} p = (0, 0) \quad \text{in } \Omega. \tag{129}$$

The case $k > 2$. Given p in Q_h, if p is locally of degree $k-2$, then the result follows from the induction hypothesis. Otherwise, there exists at least one triangle of Ω in which p is exactly of degree $k-1$. Like in the previous case, we define $\underline{v}_h = (v_1(x, y), v_2(x, y))$ as follows:

$$v_1(x,y)|_a = -\lambda^a_{AB}\lambda^a_{AE}||\operatorname{grad} p||_0 L^a_{k-2,x}\cdot\sigma, \tag{130}$$

$$v_2(x,y)|_a = -\lambda^a_{AB}\lambda^a_{AE}\frac{\partial p}{\partial y}, \tag{131}$$

$$v_1(x,y)|_b = -\lambda^b_{ED}\lambda^b_{BD}||\operatorname{grad} p||_0 L^b_{k-2,x}\cdot\sigma - \lambda^b_{ED}\lambda^b_{EB}\frac{\partial p}{\partial x}, \tag{132}$$

$$v_2(x,y)|_b = -\lambda^b_{ED}\lambda^b_{BD}\frac{\partial p}{\partial y} - \lambda^b_{ED}\lambda^b_{EB}||\operatorname{grad} p||_0 L^b_{k-2,y}\cdot\tau, \tag{133}$$

$$v_1(x,y)|_c = -\lambda^c_{BC}\lambda^c_{CD}\frac{\partial p}{\partial x}, \tag{134}$$

$$v_2(x,y)|_c = -\lambda^c_{BC}\lambda^c_{CD}||\operatorname{grad} p||_0 L^c_{k-2,y}\cdot\tau, \tag{135}$$

with the same assumption on σ and τ, so that the terms

$$H = \sigma||\operatorname{grad} p||_0\left(\int_a \lambda^a_{AB}\lambda^a_{AE}L^a_{k-2,x}\cdot\frac{\partial p}{\partial x} + \int_b \lambda^b_{ED}\lambda^b_{BD}L^b_{k-2,x}\cdot\frac{\partial p}{\partial x}\right), \tag{136}$$

$$K = \tau||\operatorname{grad} p||_0\left(\int_b \lambda^b_{EB}\lambda^b_{ED}L^b_{k-2,y}\cdot\frac{\partial p}{\partial y} + \int_c \lambda^c_{BC}\lambda^c_{CD}L^c_{k-2,y}\cdot\frac{\partial p}{\partial y}\right) \tag{137}$$

are nonnegative. The same arguments as for $k = 2$, together with the described normalization of the Legendre polynomials, show that $\underline{v}_h$ belongs to V_h.

In order to conclude the proof, we need show that if $|||\operatorname{grad} p||| = 0$ then the degree of $\operatorname{grad} p$ is strictly less than $k-2$. As before, $|||\operatorname{grad} p||| = 0$ implies

$$\frac{\partial p}{\partial y} = 0 \quad \text{in } a, \tag{138}$$

$$\operatorname{grad} p = 0 \quad \text{in } b, \tag{139}$$

$$\frac{\partial p}{\partial x} = 0 \quad \text{in } c, \tag{140}$$

$$H = K = 0. \tag{141}$$

The last equalities imply

$$\int_a \lambda^a_{AB}\lambda^a_{AE}L^a_{k-2,x}\cdot\frac{\partial p}{\partial x} = 0 \tag{142}$$

and

$$\int_c \lambda^c_{BC}\lambda^c_{CD}L^c_{k-2,y}\cdot\frac{\partial p}{\partial y} = 0 \tag{143}$$

It follows that the degree of $\operatorname{grad} p$ is strictly less than $k-2$ in contrast to our assumption.

Remark 8.2. The proof of the theorem shows that the continuity hypothesis on the pressure space Q_h can be weakened up to require that q_h is only continuous on triplets of elements.

We conclude this subsection by stating the three-dimensional analogous to the previous theorem and by recalling the main argument of the proof presented in [14].

Theorem 8.2. *Let Ω be a polyhedral domain and $\mathcal{T}_h$ a regular sequence of decompositions of it into tetrahedra. Assume that every tetrahedron has at least one internal vertex. Then the choice $V_h = (\mathfrak{L}^1_k \cap H^1_0(\Omega))^3$ and $Q_h = \mathfrak{L}^1_{k-1}$ satisfies the inf–sup condition* (20) *for any $k \geq 2$.*

Proof. We shall make use of the macroelement technique presented in Sect. 4.5. In particular, we shall use Proposition 4.9 and the comments included in Remark 4.7.

We consider an overlapping macroelement partition of $\mathcal{T}_h$ as follows: for each internal vertex x_0 we define a corresponding macroelement M_{x_0} by collecting all elements which touch x_0. Thanks to the regularity assumptions on the mesh, we only have to show that the macroelement condition (79) holds true (see, in particular, Remark 4.7).

Let us consider an element $K \in M = M_{x_0}$ and an edge e of K which touches x_0. With a suitable choice of the coordinate system, we can suppose that the direction of e coincides with that of the x axis. With the notation of Sect. 4.5 we shall show that a function in K_M cannot contain functions which depend on x in K. Namely, given a function $p \in Q_{0,M}$, we can define a function $\underline{v} \in V_{0,M}$ as follows.

$$\underline{v} = \left(-\lambda_{1,i}\lambda_{2,i} \frac{\partial p}{\partial x}, 0, 0 \right) \qquad \text{in } K_i,$$

where K_i is a generic element of M sharing the edge e with K and $\lambda_{j,i}$, $j = 1, 2$, are the barycentric coordinates of K_i associated with the two faces of K_i which do not touch e. On the remaining elements, each component of $\underline{v}$ is set equal to zero. It is clear that $\underline{v}$ is a kth-order polynomial in K_i and, since p is continuous in M, $\partial p/\partial x$ is continuous across the faces which meet at e and the function $\underline{v}$ is continuous as well. Hence, $\underline{v}$ belongs to $V_{0,M}$.

From the definition of $Q_{0,M}$ it turns out that

$$0 = \int_M p \operatorname{div} \underline{v} = -\int_M \operatorname{grad} p \cdot \underline{v} = \sum_i \int_{K_i} \lambda_{1,i}\lambda_{2,i} \left| \frac{\partial p}{\partial x} \right|^2$$

The last relation implies that p does not depend on x in K_i for any i and, in particular, in K. On the other hand, we can repeat the same argument using as e the other two edges of K meeting at x_0 and, since the directions of the three used edges are independent, we obtain that p is constant in K.

Remark 8.3. From the previous proof we can deduce that the hypotheses on the triangulation can be weakened, by assuming that each tetrahedron has at least three edges which do not lie on the boundary of Ω and which are not in the same plane. On the other hand, given a generic mesh of tetrahedra, it is not difficult to add suitable elements in order to meet the requirements of the previous theorem.

Remark 8.4. The main argument in the proof of the previous theorem is the straightforward generalization of the two-dimensional case. Indeed, the proof of Theorem 8.1 could be carried out using the macroelement technique as well.

9 Nearly Incompressible Elasticity, Reduced Integration Methods and Relation with Penalty Methods

9.1 Variational Formulations and Admissible Discretizations

Let us now turn our attention on problems associated with approximations of nearly incompressible materials. Considering, to make things simpler, a problem with homogeneous Dirichlet conditions and the standard variational principle

$$\inf_{\underline{v}\in(H_0^1(\Omega))^2} \mu \int_\Omega |\underline{\underline{\varepsilon}}(\underline{v})|^2 \, dx + \frac{\lambda}{2} \int_\Omega |\operatorname{div} \underline{v}|^2 \, dx - \int_\Omega \underline{f} \cdot \underline{v} \, dx, \tag{144}$$

it can be noticed that this problem is closely related to a penalty method to solve the Stokes problem.

It was soon recognized in practice that a brute force use of (144) could lead, for large values of λ, to bad results, the limiting case being the locking phenomenon that is an identically zero solution. A cure was found in using a reduced (that is inexact) numerical quadrature when evaluating the term $\lambda \int_\Omega |\operatorname{div} \underline{v}|^2 \, dx$ associated with compressibility effects. We refer the reader to the papers of [50] and [9] for a discussion of the long history of this idea. We shall rather develop in details on this example the relations of reduced integrations and mixed methods and try to make clear to what extent they may be claimed to be equivalent. For this we first recall that problem (144) can be transformed by a straightforward application of duality techniques into a saddle point problem

$$\inf_{\underline{v}} \sup_{q} \mu \int_\Omega |\underline{\underline{\varepsilon}}(\underline{v})|^2 \, dx - \frac{2}{2\lambda} \int_\Omega |q|^2 \, dx + \int_\Omega q \, \operatorname{div} \underline{v} \, dx - \int_\Omega \underline{f} \cdot \underline{v} \, dx \tag{145}$$

for which optimality conditions are, denoting $(\underline{u}, p)$ the saddle point,

$$\mu \int_\Omega \underline{\underline{\varepsilon}}(\underline{u}) : \underline{\underline{\varepsilon}}(\underline{v}) \, dx + \int_\Omega p \, \operatorname{div} \underline{v} \, dx = \int_\Omega \underline{f} \cdot \underline{v} \, dx, \forall \underline{v} \in (H_0^1(\Omega))^2 \tag{146}$$

$$\int_\Omega \operatorname{div} \underline{u} \, q \, dx = \frac{1}{\lambda} \int_\Omega pq \, dx, \forall q \in L^2(\Omega). \tag{147}$$

This is obviously very close to a Stokes problem and is also an example of a problem of the following nature

$$a(u, v) + b(v, p) = (f, v), \forall v \in V, \; u \in V, \tag{148}$$

$$b(u, q) - c(p, q) = (g, q), \forall q \in Q, \; p \in Q. \tag{149}$$

We can then derive that an approximation of (146) and (147) (that is a choice of an approximation for both $\underline{u}$ and p) which leads to error estimates independent of λ must be a good approximation for Stokes problem. The preceding sections of this chapter therefore give us a good idea of what should (or should not) be used as an approximation. What we shall now see is that reduced integration methods correspond to *an implicit choice* of a mixed approximation. The success of the reduced integration method will thus rely on the qualities of this underlying mixed method.

9.2 Reduced Integration Methods

Let us consider a (more or less) standard approximation of the original problem (144). An exact evaluation of the "penalty term" $\lambda \int_\Omega |\operatorname{div}\ \underline{v}|^2 dx$ means that for λ large one tries to get an approximation of $\underline{u}$ which is *exactly* divergence-free. But as we have already seen few finite elements can stand such a condition that will in most cases lead to locking phenomenon due to overconstraining. In a mixed formulation one relaxes the incompressibility condition by the choice of the approximation for p. Let us now see how this will be translated as a reduced integration method at least in some cases. Let us then consider $V_h \subset V = (H_0^1(\Omega))^2,\ Q_h \subset Q = L^2(\Omega)$, these approximation spaces being built from finite elements defined on a partition of Ω. On each element K, let there be given a set of k points x_i and weights ω_i defining a numerical quadrature formula

$$\int_K f(x)\ dx = \sum_{i=1}^{k} \omega_i\ f(x_i). \tag{150}$$

Remark 9.1. It will be convenient to define the numerical quadrature on a reference element K and to evaluate integrals by a change of variables.

$$\int_K f(x)\ dx = \int_{\hat{K}} f(\hat{x})\ J(\hat{x})\ d\hat{x} = \sum_{i=1}^{k} \omega_1\ f(\hat{x}_i)\ J(\hat{x}_i). \tag{151}$$

The presence of the Jacobian $J(x)$ should be taken into account when discussing the precision of the quadrature rule on K.

Let us now make the hypothesis that for $\underline{v}_h \in V_h$ and $p_h,\ q_h \in Q_h$, one has exactly

$$\int_K q_h\ \operatorname{div}\ \underline{v}_h\ dx = \sum_{i=1}^{k} \omega_i\ \hat{q}_h(\hat{x}_i)\widehat{\operatorname{div}\ \underline{v}_h}(\hat{x}_i)\ J(\hat{x}_i) \tag{152}$$

and

$$\int_K p_h\ q_h\ dx = \sum_{k=1}^{k} \omega_i\ \hat{p}_h(\hat{x}_i)\ \hat{q}_h(\hat{x}_i)\ J(\hat{x}_i). \tag{153}$$

Let us now consider the discrete form of (147)

$$\int_\Omega \operatorname{div}\ \underline{u}_h\ q_h\ dx = \frac{1}{\lambda} \int_\Omega p_h\ q_h\ dx,\ \forall q_h \in Q_h. \tag{154}$$

When the space Q_h is built from discontinuous functions, this can be read element by element

$$\int_K q_h\ \operatorname{div}\ \underline{u}_h\ dx = \frac{1}{\lambda} \int_K p_h\ q_h\ dx,\ \forall q_h \in Q_h, \tag{155}$$

so that using (152) and (153) one gets

$$\hat{p}_h(\hat{x}_i) = \lambda \widehat{\operatorname{div}\ \underline{u}_h}(\hat{x}_i) \text{ or } p_h(x_i) = \lambda \operatorname{div}\ u_h(x_i). \tag{156}$$

Formula (151) can in turn be used in the discrete form of (146) which now gives

$$\begin{cases} 2\mu \int_\Omega \underline{\underline{\varepsilon}}(\underline{u}_h) : \underline{\underline{\varepsilon}}(\underline{v}_h)\, dx + \lambda \sum_K \Big(\sum_{i=1}^k \omega_i\, J(\hat{x}_i)(\widehat{\operatorname{div}\ \underline{u}_h}(\hat{x}_i)(\widehat{\operatorname{div}\ \underline{v}_h}(\hat{x}_i))\Big) \\ \qquad\qquad = \int_\Omega \underline{f} \cdot \underline{v}_h\, dx. \end{cases} \tag{157}$$

In general the term $\sum_K \Big(\sum_{i=1}^k \omega_i\ J(\hat{x}_i)(\widehat{\operatorname{div}\ \underline{u}_h}(\hat{x}_i)(\widehat{\operatorname{div}\ \underline{v}_h}(\hat{x}_i))\Big)$ *is not* an exact evaluation of $\int_\Omega \operatorname{div}\ \underline{u}_h\ \operatorname{div}\ \underline{v}_h\ dx$ and reduced integration is effectively introduced. In the case where (152) and (153) hold there is a perfect equivalence between the mixed method and the use of reduced integration. Whatever will come from one can be reduced to the other one. It will however not be in general possible to get equalities (152) and (153) so that a further analysis will be needed. But we shall first consider some examples of this complete equivalence case.

Example 9.1. Let us consider the $Q_1 - P_0$ approximation on a *rectangle* and a one-point quadrature rule. It is clear that $\operatorname{div}\ \underline{u}_h \in P_1(K)$ and is integrated exactly. In the same way a one-point rule is exact for $\int_\Omega p_h\ q_h\ dx$ whenever $p_h,\ q_h \in P_0(K)$. There is thus a perfect equivalence between reduced integration and the exact penalty method defined by (154).

Example 9.2. We now consider again the same $Q_1 - P_0$ element on a general quadrilateral. To show that we still have equivalence requires a somewhat more delicate analysis. Indeed at first sight the quadrature rule is not exact for $\int_{\hat{K}} \widehat{\operatorname{div}\ \underline{u}_h}\ \ J_K(\hat{x})\ \ d\hat{x}$. Let us however consider in detail the term $\widehat{\operatorname{div}\ \underline{u}_h} = \widehat{\frac{\partial u_1}{\partial x_1}} + \widehat{\frac{\partial u_2}{\partial x_2}}$. Let $B = DF$ be the Jacobian matrix of the transformation F from $\hat{K}$ into K. Writing explicitly

$$F = \begin{cases} a_0 + a_1\hat{x} + a_2\hat{y} + a_3\hat{x}\hat{y} \\ b_0 + b_1\hat{x} + b_2\hat{y} + b_3\hat{x}\hat{y} \end{cases} \tag{158}$$

one has

$$B = \begin{pmatrix} a_1 + a_3\hat{y} & a_2 + a_3\hat{x} \\ b_1 + b_3\hat{y} & b_2 + b_3\hat{x} \end{pmatrix} \tag{159}$$

so that we get

$$B^{-1} = \frac{1}{J(\hat{x})} \begin{pmatrix} b_2 + b_3\hat{x} & -a_2 - a_3\hat{x} \\ -b_1 - b_3\hat{y} & a_1 + a_3\hat{y} \end{pmatrix}. \tag{160}$$

But

$$\widehat{\frac{\partial u_1}{\partial x_1}} = \Big(\frac{\partial \hat{u}_1}{\partial \hat{x}_1}(b_2 + b_3\hat{x}) - \frac{\partial \hat{u}_1}{\partial \hat{x}_2}(b_1 + b_3\hat{y}) \Big) \frac{1}{J(\hat{x})}, \tag{161}$$

$$\widehat{\frac{\partial u_2}{\partial x_2}} = \Big(\frac{\partial \hat{u}_2}{\partial \hat{x}_1}(-a_2 - a_3\hat{x}) + \frac{\partial \hat{u}_2}{\partial \hat{x}_2}(a_1 + a_3\hat{y}) \Big) \frac{1}{J(\hat{x})}. \tag{162}$$

When computing $\int_{\hat{K}} \widehat{\operatorname{div}\ \underline{u}_h}\ J(\hat{x})\ d\hat{x}$, Jacobians cancel and one is left with the integral of a function which is linear in each variable and which can be computed exactly by a one-point formula.

Example 9.3. Using a four-point integration formula on a straight-sided quadrilateral can be seen as in the previous example to be exactly equivalent to a $Q_2 - Q_1$ approximation [8, 9].

The above equivalence is however not the general rule. Consider the following examples.

Example 9.4. We want to use a reduced integration procedure to emulate the Crouzeix–Raviart $P_2 - P_1$ element. To define a P_1 pressure, we need three integration points which can generate a formula that will be exact for second degree polynomials (but not more). The bubble function included in velocity however makes $\operatorname{div}\ \underline{u}_h \in P_2(K)$ and $\int_K \operatorname{div}\ \underline{u}_h\ q_h dx$ will not be evaluated exactly.

Example 9.5. A full isoparametric $Q_2 - Q_1$ element is not equivalent to its four-point reduced integration analogue.

Example 9.6. A $Q_2 - P_0$ approximation is not, even on rectangles, equivalent to a one-point reduced integration method for $\operatorname{div} \underline{u}_h$ contains second-order term which are not taken into account by a one-point quadrature.

9.3 Effects of Inexact Integration

If we now consider into more details the cases where a perfect equivalence does not hold between the mixed method and some reduced integration procedure we find ourselves in the setting of nonconforming approximation. In particular $b(\underline{v}_h, q_h)$ is replaced by an approximate bilinear form $b_h(\underline{v}_h, q_h)$. We shall suppose to simplify that the scalar product on Q_h is exactly evaluated. Two questions must then be answered.

— Does $b_h(.,.)$ satisfy the inf–sup condition?
— Do error estimates still hold without loss of accuracy?

Example 9.7. We in fact come back to Example 9.6 and study on a rectangular mesh, the $Q_2 - P_0$ approximation (see Sect. 6.4) with a one-point quadrature rule. This is not, as we have said, equivalent to the standard $Q_2 - P_0$ approximation. We now want to check, using Proposition 4.1, that it satisfies the inf–sup condition. We thus have to build a continuous operator (in $H^1(\Omega)$-norm) such that

$$\int_\Omega \operatorname{div}\ \underline{u}_h\ q_h\ dx = \sum_K [(\operatorname{div}\ \Pi_h \underline{u}_h)(M_{0,K}) q_K]\ \text{area}(K) \tag{163}$$

where $M_{0,K}$ is the barycenter of K and q_K the restriction of q_h to K. We can restrict our analysis to one element as q_h is discontinuous and we study both sides of equality (163). We have of course, taking $q_K = 1$,

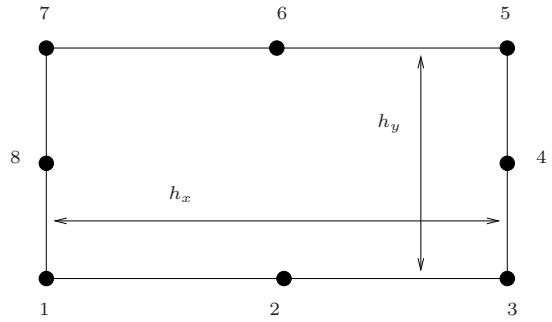

Fig. 16. A rectangle

$$\int_K \text{div } \underline{u}_h \, dx = \int_{\partial K} \underline{u}_h \cdot \underline{n} \, d\sigma. \tag{164}$$

Using the numbering of Fig. 16 and denoting by u_i, v_i the horizontal and vertical components of velocity at node i, we can write (164) by Simpson's quadrature rule in the form

$$\begin{cases} \displaystyle\int_K \text{div } \underline{u}_h \, dx = \frac{h_y}{6}[u_5 + 4u_4 + u_3] - \frac{h_y}{6}[u_1 + 4u_8 + u_7] \\ \qquad\qquad + \dfrac{h_x}{6}[v_7 + 4v_6 + v_5] - \dfrac{h_x}{6}[v_1 + 4v_2 + v_3]. \end{cases} \tag{165}$$

If we write

$$u_4 = \frac{u_5 + u_3}{2} + \hat{u}_4, \; u_8 = \frac{u_1 + u_7}{2} + \hat{u}_8 \tag{166}$$

$$v_6 = \frac{v_5 + v_7}{2} + \hat{v}_6, \; v_2 \; = \frac{v_1 + v_3}{2} + \hat{v}_2 \tag{167}$$

where $\hat{u}_4, \hat{u}_6, \hat{v}_6$ and $\hat{v}_2$ are corrections with respect to a bilinear interpolation we may rewrite (165) as

$$\begin{cases} \displaystyle\int_K \text{div } \underline{u}_h \, dx = \frac{h_y}{2}[u_5 + u_3 + \frac{4}{3}\hat{u}_4] - \frac{h_y}{2}[u_1 + u_7 + \frac{4}{3}\hat{u}_8] \\ \qquad\qquad + \dfrac{h_y}{2}[v_7 + v_5 + \dfrac{4}{3}\hat{v}_6] - \dfrac{h_x}{2}[v_1 + v_3 + \dfrac{4}{3}\hat{v}_2]. \end{cases} \tag{168}$$

On the other hand area (K) $\text{div } \underline{u}_h(M_{0,K})$ can be seen to be equal to

$$\begin{cases} \dfrac{h_y}{2}[u_5 + u_3 + 2\hat{u}_4] - \dfrac{h_y}{2}[u_1 + u_7 + 2\hat{u}_8] \\ -\dfrac{h_x}{2}[u_7 + v_5 + 2\hat{v}_6] - \dfrac{h_x}{2}[v_1 + v_3 + 2\hat{u}_2]. \end{cases} \tag{169}$$

If we thus split $\underline{u}_h$ into a bilinear part $\underline{u}_h^0$ and a mid-point correction part $\underline{\hat{u}}_h$, one can define $\Pi_h \underline{u}_h$ by setting

$$\begin{cases} (\Pi_h \underline{u}_h)^0 = \underline{u}_h^0, \\ (\widehat{\Pi_h \underline{u}_h}) = \dfrac{2}{3} \hat{\underline{u}}_h. \end{cases} \tag{170}$$

Equality (164) will then hold and (170) is clearly continuous with a continuity constant independent of h.

Example 9.8. We come back to Example 9.4 that is a three-point quadrature rule used in conjunction with the Crouzeix–Raviart element. We shall not give the analysis in details but only sketch the ideas. The problem is again to check that the inf–sup condition holds through Proposition 4.1. As the quadrature rule *is exact* when q_h is *piecewise constant*, the obvious idea is to build $\Pi_h \underline{u}_h$ by keeping the trace of $\underline{u}_h$ on ∂K and *only modifying the coefficients of the bubble functions*. This can clearly be done. Continuity is now to be checked and the proof is essentially the same as the standard proof of the inf–sup condition (Sect. 7.2).

Example 9.9 (A modified $Q_1 - P_0$ element). We now present a puzzling example of an element which is stable but for which convergence is tricky due to a consistency error term. We have here a case where using a one-point quadrature rule will change the situation with respect to the inf–sup condition. In fact it will make a stable element from an unstable one but will also introduce an essential change in the problem. The departure point is thus the standard $Q_1 - P_0$ element which, as we know, does not satisfy the inf–sup condition. We now make it richer by adding to velocity $\underline{u}_h|_K = \{u_1, u_2\}$ what we shall call wave functions. On the reference element $\hat{K} =]-1, 1[\times]-1, 1[$, those functions are defined by

$$\begin{cases} w_1 = \hat{x}\ b_2(\hat{x}, \hat{y}), \\ w_2 = \hat{y}\ b_2(\hat{x}, \hat{y}), \end{cases} \tag{171}$$

where $b_2(\hat{x}, \hat{y}) = (1 - \hat{x}^2)(1 - \hat{y}^2)$ is the Q_2 bubble function. If we now consider

$$\hat{\underline{u}}_h|_K = \{u_1 + \alpha_K w_1, u_2 + \alpha_K w_2\} = \underline{u}_h|_K + \alpha_K \underline{w}_K, \tag{172}$$

we obtain a new element with an internal degree of freedom. The wave functions that we added vanish on the boundary and nothing is changed for the stability of the mixed method with exact integration. If we rather use a one-point quadrature rule, things become different. We shall indeed check that the modified bilinear form $b_h(\underline{\hat{v}}_h, q_h)$ satisfies the inf–sup condition. We thus have to show that

$$\sup_{\hat{\underline{u}}_h} \frac{\sum\limits_K \operatorname{div}\ \hat{\underline{u}}_h(M_{0,K}) p_K\ h_K^2}{\|\hat{\underline{u}}_h\|_1} \geq k_0\ |p_h|_0. \tag{173}$$

This is easily checked by posing on K (we suppose a rectangular mesh to simplify)

$$\hat{\underline{u}}_h|_K = h_K\ p_K \underline{w}_K. \tag{174}$$

We then have $\operatorname{div}\ \hat{\underline{u}}_h = p_h$ and

$$\|\underline{\hat{u}}_h\|_{1,K} = h\, p_K\, \|\underline{w}_K\|_{1,K}, \tag{175}$$

which implies

$$\|\underline{\hat{u}}_h\|_1 \leq c\, |p_h|_0, \tag{176}$$

and (173) follows. A remarkable point is that even the hydrostatic mode has disappeared. This is an indication that something incorrect has been introduced in the approximation. An analysis of *consistency error* indeed shows that usual error estimates fail and that we are actually approximating a continous problem in which the incompressibility condition has been replaced by $\operatorname{div} u + kp = 0$ where $k = 1575/416$. We then see that if in general for Stokes problem, making the space of velocities richer improves (at least does not reduce) the quality of the method, this fact can become false when numerical integration is used.

Let us now turn our attention to the problem of error estimation. From [24] all we have to do is to estimate the consistency terms

$$\sup_{v_h} \frac{|b_h(v_h, p) - b_h(v_h, p)|}{\|v_h\|_V} \tag{177}$$

and

$$\sup_{q_h} \frac{|b(u, q_h) - b_h(u, q_h)|}{\|q_h\|_0}. \tag{178}$$

We thus have to estimate quadrature errors. It would be out of purpose to enter into details and we refer the reader to [27, 28] where examples of such analysis are presented exhaustively. The first step is to transform (177) into a form which is sometimes more tractable. We may indeed write

$$\begin{cases} b(v_h, p) - b_h(v_h, p) = (b(v_h, p - q_h) - b_h(v_h, p - q_h)) \\ \qquad\qquad\qquad\qquad + (b(v_h, q_h) - b_h(v_h, q_h)) \end{cases} \tag{179}$$

and

$$\begin{cases} b(u, q_h) - b_h(u, q_h) = (b(u - v_h, q_h) - b_h(u - v_h, q_h)) \\ \qquad\qquad\qquad\qquad + (b(v_h, q_h) - b_h(v_h, q_h)). \end{cases} \tag{180}$$

The first parenthesis in the right-hand side of (179) and (180) can be reduced to an approximation error. The second parenthesis implies only polynomials.

Let us therefore consider (180) for the three approximations introduced above. (Coming back to the notations of the present section). For the Crouzeix–Raviart triangle taking $\underline{v}_h$ the standard interpolate of $\underline{u}$ makes the second parenthesis vanish while the first yields an $O(h)$ estimate. For the two other approximations taking $\underline{v}_h$ to be a standard bilinear approximation of $\underline{u}$ makes the second parenthesis vanish while the first yields on $O(h)$ estimate, which is the best that we can hope anyway. The real trouble is therefore with (177) with or without (179). In the case of the Crouzeix–Raviart triangle, we can use directly (177) and the following result of [27, 28], (Theorem IV.1.5).

Proposition 9.1. *Let $f \in W_{k,q}(\Omega),\ p_k \in P_k(K)$ and denote $E_k(fp_k)$ the quadrature error on element K when numerical integration is applied to fp_k. Let us suppose that $E_K(\hat{\phi}) = 0,\ \forall \hat{\phi} \in P_{2k-2}(K)$ then one has*

$$|E_K(fp_k)| \leq ch_K^k\ (meas(K))^{\frac{1}{2}-\frac{1}{q}} |f|_{k,q,K} |p_k|_1. \tag{181}$$

Taking $k = 2, q = \infty$ and using the inverse inequality to go from $|p_k|_1$ to $|p_k|_0$ one gets an $O(h^2)$ estimate for (177).

The two other approximations cannot be reduced to Proposition 9.1 and must be studied through (179). We must study a term like

$$\sup_{v_h} \frac{|b(v_h, q_h) - b_h(v_h, q_h)|}{\|v_h\|_1}. \tag{182}$$

This can at best be *bounded*. For instance in the case of the $Q_2 - P_0$ approximation we can check by hand that the quadrature error on K reduces to $h_K^3\ |\operatorname{div}\ \underline{v}_h|_{2,K}\ p_k$.

10 Divergence-Free Basis, Discrete Stream Functions

We have dealt in this note with the mixed formulation of the Stokes problem and we have built finite element approximations in which discrete divergence-free functions approximate the continuous ones. It is sometimes useful to consider directly the constrained minimization problem

$$\inf_{\underline{v}_0 \in V_0} \frac{1}{2} \int_\Omega |\underline{\underline{\varepsilon}}(\underline{v}_0)|^2\, dx - \int_\Omega \underline{f} \cdot \underline{v}_0\, dx, \tag{183}$$

where V_0 is the subspace of divergence-free functions. In this subspace we have a standard minimization problem and the discrete form would lead to a positive definite linear system. Indeed the solution of problem (183) satisfies the variational equation,

$$\int_\Omega \underline{\underline{\varepsilon}}(\underline{u}_0) : \underline{\underline{\varepsilon}}(\underline{v}_0)\, dx = \int_\Omega \underline{f} \cdot \underline{v}_0\, dx,\ \forall \underline{v}_0 \in V_0, \underline{u}_0 \in V_0. \tag{184}$$

In the discrete problem, if one knows a basis $\{\underline{w}_0, \ldots, \underline{w}_m\}$ of V_{0h} the solution is reduced to the solution of the linear system

$$A_0\ U_0 = F_0, \tag{185}$$

where

$$a_{ij}^0 = \int_\Omega \underline{\underline{\varepsilon}}(\underline{w}_i) : \underline{\underline{\varepsilon}}(\underline{w}_j)\, dx, \quad f_i^0 = \int_\Omega \underline{f} \cdot \underline{w}_i\, dx, \tag{186}$$

and

$$A_0 = \{a_{ij}^0\},\ F_0 = \{f_i^0\}. \tag{187}$$

Building a basis for the divergence-free subspace could therefore lead to a neat reduction of computational costs: pressure is eliminated, along with a certain amount

of velocity degrees of freedom. System (185) is smaller than the original one. It must however be noted that with respect to the condition number, (185) is behaving like a fourth-order problem, which makes its practical usefulness often dubious. As to pressure, it can be recovered a posteriori (see [25, 26]).

The construction of such a basis is not however a very popular method and is considered as a hard task although it has been numerically implemented (see [43, 65, 44]).

As we shall see the two-dimensional case is quite readily handled in many cases. The degrees of freedom can be associated with those of a discrete stream function. The three-dimensional problem is harder to handle: a generating system can often easily be found but the construction of a basis requires the elimination of some degrees of freedom in a not so obvious way.

We shall also consider rapidly a numerical procedure, related to static condensation that will require a partly divergence-free basis.

Finally we want to emphasize that the construction which we describe will make sense only if the finite element approximation is good so that the previous analysis is still necessary even if it might seem to be bypassed.

We first consider a simple example of a divergence-free basis.

Example 10.1 (The nonconforming $P_1 - P_0$ element). We consider the classical nonconforming element introduced in [31] (cf. Sect. 6.3) in which mid-side nodes are used as degrees of freedom for velocity. This generates a piecewise linear nonconforming approximation; pressure is taken constant on each element (Fig. 17). The restriction to an element K of $\underline{u}_h \in V_h$ is then exactly divergence-free and is therefore locally the curl of a quadratic polynomial. This discrete stream function cannot be continuous on interfaces but must have continuous derivatives at mid-side points: it can be built from Morley's triangle. The degrees of freedom of the divergence-free basis can be associated to the degrees of freedom of this nonconforming stream function (Fig. 18). This assigns a basis function to each vertex and to each mid-side node. They are depicted schematically in Fig. 19. One observes a general pattern: divergence-free functions are made from small vortices.

Remark 10.1. The kind of basis obtained in the previous example is typical of a domain without holes with homogeneous Dirichlet boundary conditions. Whenever a hole is present, an extra basis function must be added in order to ensure circulation around the hole (Fig. 20). This function is not local.

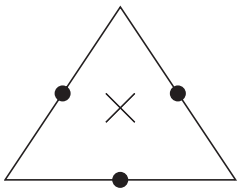

Fig. 17. Nonconforming element

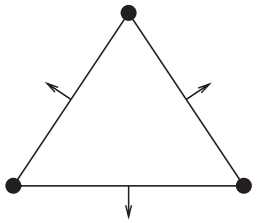

Fig. 18. Nonconforming stream function

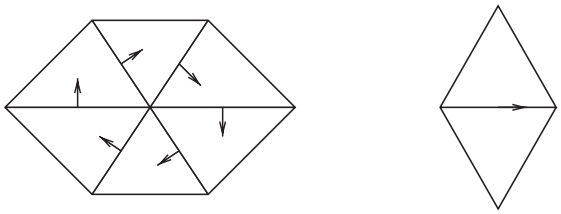

Fig. 19. Basis functions for a divergence free P_1–P_0 nonconforming element

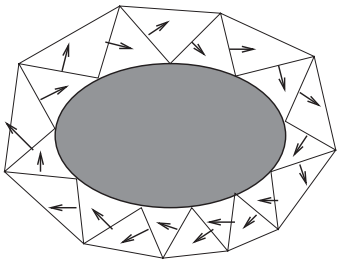

Fig. 20. Divergence free function around a hole

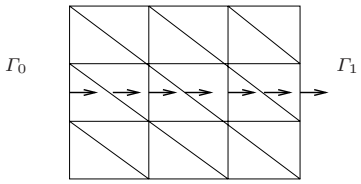

Fig. 21. Divergence free function with different boundary conditions

In the same way when the flow is entering on a part Γ_0 of $\partial\Omega$ and outgoing on a part Γ_1, a basis function must be provided to link those parts and to thus take into account the potential part of the flow (Fig. 21).

We now consider a conforming approximation, namely the popular $Q_2 - P_1$ element (see Sect. 6.4).

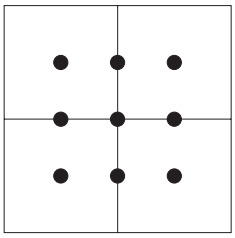

Fig. 22. A 2×2 macroelement

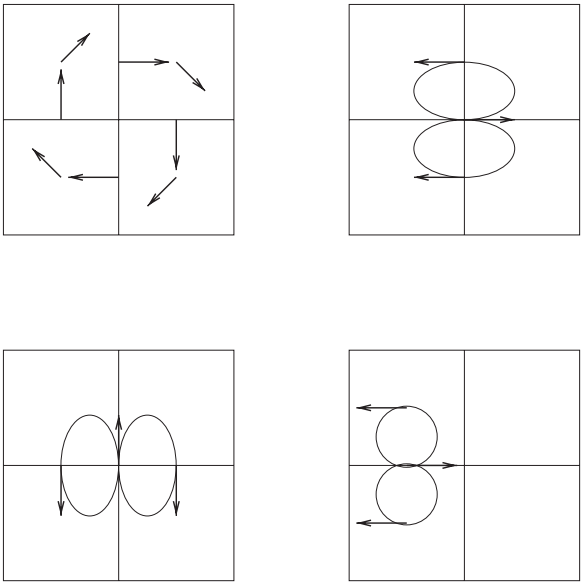

Fig. 23. Divergence-free functions

Example 10.2 (The conforming $Q_2 - P_1$ element). We shall sketch in this example the construction of a divergence-free basis for the $Q_2 - P_1$ element. To make things simple we shall assume that the mesh is formed of 2×2 macroelements. The general case can easily be deduced. Let us first look for divergence-free (in the discrete sense of course) functions with their support on a macroelement. We have 18 degrees of freedom for velocity (Fig. 22) linked by $(12 - 1) = 11$ linear constraints. This leaves seven linearly independent functions which can be described by the diagrams of Fig. 23.

Three of them are associated with each vertex and one to each mid-side node. It must be noted that internal nodes are no longer degrees of freedom.

Remark 10.2. The "divergence-free" functions described above cannot be taken as the curl of a stream-function as they are not exactly divergence-free. However a discrete stream-function can nevertheless be built. Its trace on ∂K can be totally

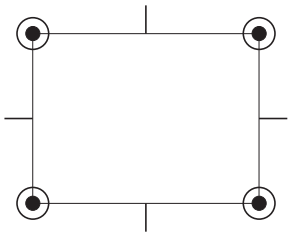

Fig. 24. Adini's element

determined by integrating $\underline{u}_h \cdot \underline{n}$ along the boundary. As the flow is conserved at element level this defines $\psi_h|_{\partial K}$ which is a piecewise third degree polynomial such that $\frac{\partial \psi_h}{\partial \tau} = \underline{u}_h \cdot \underline{n}$. This stream-function could be built from the element of Fig. 24 (Adini's element) but $\underline{u}_h$ must be deduced by taking a *discrete curl operation*.

Other methods which have been studied for elasticity problems can be extended to Stokes problem. For instance, the Hellan–Hermann–Johnson mixed method for plate bending has been extended to the $\psi - \omega$ formulation for Stokes by [22].

11 Other Mixed and Hybrid Methods for Incompressible Flows

We have considered in this chapter only the most standard applications to the Stokes problem using primitive variables. This is not by far the only possibility; the $\psi - \omega$ decomposition of the biharmonic problem, for instance, can be applied to a Stokes problem. Indeed any divergence-free functions $\underline{u} \in (H_0^1(H))^2$ can be written in the form

$$\underline{u} = \operatorname{curl} \psi, \ \psi \in H_0^2(\Omega). \tag{188}$$

From (188) we get

$$\operatorname{curl} \underline{u} = \omega = -\triangle \psi. \tag{189}$$

On the other hand, taking the curl of equation (1) gives

$$-\triangle \omega = \operatorname{curl} \underline{f} = f_1. \tag{190}$$

This procedure can be extended to the Navier–Stokes equation (indeed in many ways) including, if wanted, some upwinding procedure for the nonlinear terms (see [40, 47]). The reader will find a fairly complete study of such procedures in [42], [53]. It must be noted that the simplest case of such a procedure, using for ψ_h a bilinear approximation yields as an approximation of $\underline{u}$ the famous MAC cells (Fig. 25).

Indeed this is nothing but the space $RT_{[0]}$ for which the subspace of divergence-free functions can be obtained from a bilinear stream-function. The Hellan–Hermann–Johnson mixed method for elasticity can also be applied to the Stokes problem with $\underline{u}_h$ chosen in some approximation of $H(\operatorname{div}, \Omega)$. A direct approach precludes to use a symmetric tensor and forces to use $\underline{\operatorname{grad}}\, \underline{u}$ instead of

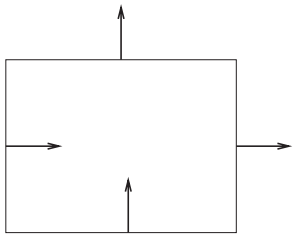

Fig. 25. MAC cell

$\underline{\underline{\varepsilon}}(\underline{u})$ as dual variable [4]. This difficulty has been circumvented by [51] by enriching the spaces by the trick of [1] or [2] or [20].

Finally it must be said that dual hybrid methods have been applied by [7] to the Stokes problem. This generates elements which are defined only by the traces at the boundaries and for which internal values can be chosen arbitrarily. This can be seen as the ultimate case of enrichment by bubble functions: enriching by a (potentially infinite dimensional) space enables to use exactly divergence-free function, provided the inf–sup condition is satisfied for *piecewise constant pressure*.

References

1. M. Amara and J.M. Thomas. Equilibrium finite elements for the linear elastic problem. *Numer. Math.*, 33:367–383, 1979.
2. D.N. Arnold, F. Brezzi, and J. Douglas. PEERS: a new mixed finite element for plane elasticity. *Jpn. J. Appl. Math.*, 1:347–367, 1984.
3. D.N. Arnold, F. Brezzi, and M. Fortin. A stable finite element for the Stokes equations. *Calcolo*, 21:337–344, 1984.
4. D.N. Arnold and J.S. Falk. A new mixed formulation for elasticity. *Numer. Math.*, 53:13–30, 1988.
5. D.N. Arnold. On nonconforming linear-constant elements for some variants of the Stokes equations. *Istit. Lombardo Accad. Sci. Lett. Rend. A*, 127(1):83–93 (1994), 1993.
6. D.N. Arnold, D. Boffi, and R.S. Falk. Approximation by quadrilateral finite elements. *Math. Comp.*, 71(239):909–922, 2002.
7. S.N. Atluri and C. Yang. A hybrid finite element for Stokes flow II. *Int. J. Numer. Methods Fluids*, 4:43–69, 1984.
8. M. Bercovier. *Régularisation duale des problèmes variationnels mixtes*. PhD thesis, Université de Rouen, 1976.
9. M. Bercovier. Perturbation of a mixed variational problem, applications to mixed finite element methods. *R.A.I.R.O. Anal. Numer.*, 12:211–236, 1978.
10. M. Bercovier and O.A. Pironneau. Error estimates for finite element method solution of the Stokes problem in the primitive variables. *Numer. Math.*, 33:211–224, 1977.
11. C. Bernardi and G. Raugel. Méthodes d'éléments finis mixtes pour les équations de Stokes et de Navier–Stokes dans un polygone non convexe. *Calcolo*, 18:255–291, 1981.
12. D. Boffi. Stability of higher order triangular Hood–Taylor methods for stationary Stokes equations. *Math. Models Methods Appl. Sci.*, 2(4):223–235, 1994.

13. D. Boffi. Minimal stabilizations of the $P_{k+1} - P_k$ approximation of the stationary Stokes equations. *Math. Models Methods Appl. Sci.*, 5(2):213–224, 1995.
14. D. Boffi. Three-dimensional finite element methods for the Stokes problem. *SIAM J. Numer. Anal.*, 34:664–670, 1997.
15. D. Boffi and L. Gastaldi. On the quadrilateral $Q_2 - P_1$ element for the Stokes problem. *Int. J. Numer. Methods Fluids*, 39:1001–1011, 2002.
16. D. Boffi and C. Lovadina. Analysis of new augmented Lagrangian formulations for mixed finite element schemes. *Numer. Math.*, 75(4):405–419, 1997.
17. D. Boffi, F. Brezzi, and L. Gastaldi. On the problem of spurious eigenvalues in the approximation of linear elliptic problems in mixed form. *Math. Comput.*, 69(229):121–140, 2000.
18. J.M. Boland and R.A. Nicolaides. Stability of finite elements under divergence constraints. *SIAM J. Numer. Anal.*, 20(4):722–731, 1983.
19. F. Brezzi and K.J. Bathe. A discourse on the stability conditions for mixed finite element formulations. *CMAME*, 82:27–57, 1990.
20. F. Brezzi, J. Douglas, Jr., and L.D. Marini. Recent results on mixed finite element methods for second order elliptic problems. *Vistas in applied mathematics,* 25–43, Transl. Ser. Math. Engrg., Optimization Software, New York, 1986.
21. F. Brezzi and R.S. Falk. Stability of higher-order Hood-Taylor methods. *SIAM J. Numer. Anal.*, 28(3):581–590, 1991.
22. F. Brezzi, J. Le Tellier, and T. Olier. Mixed finite element approximation for the stationary Navier–Stokes equations (in Russian). In *Viceslitelnia Metodii V. Prikladnoi Mathematiceskie*, NAUKA, Novosibirsk, 1982, pp. 96–108. Meeting INRIA, Novosibirsk.
23. F. Brezzi and J. Pitkäranta. On the stabilization of finite element approximations of the Stokes equations. In W. Hackbush, editor, *Efficient Solutions of Elliptic Systems*, *Notes on Numerical Fluid Mechanics*, vol. 10, Braunschweig, Wiesbaden, Vieweg, 1984.
24. F. Brezzi and M. Fortin. *Mixed and Hybrid Finite Element Methods*. Springer, Berlin Heidelberg New York, 1991.
25. P. Caussignac. Explicit basis functions of quadratic and improved quadratic finite element spaces for the Stokes problem. *Commun. Appl. Numer. Methods*, 2:205–211, 1986.
26. P. Caussignac. Computation of pressure from the finite element vorticity stream-function approximation of the Stokes problem. *Commum. Appl. Numer. Methods*, 3:287–295, 1987.
27. P.G. Ciarlet. *Mathematical elasticity, vol. I. Three-Dimensional Elasticity*. North-Holland, Amsterdam, 1988.
28. P.G. Ciarlet. *Mathematical elasticity, vol. II. Theory of Plates*. North-Holland, Amsterdam, 1997.
29. J.F. Ciavaldini and J.C. Nédélec. Sur l'élément de Fraeijs de Veubeke et Sander. *R.A.I.R.O. Anal. Numer.*, 8:29–45, 1974.
30. P. Clément. Approximation by finite element functions using local regularization. *R.A.I.R.O. Anal. Numer.*, 9:77–84, 1975.
31. M. Crouzeix and P.A. Raviart. Conforming and nonconforming finite element methods for solving the stationary Stokes equations. *R.A.I.R.O. Anal. Numer.*, 7:33–76, 1973.
32. G. Duvaut and J.L. Lions. *Les inéquations en mécanique et en physique*. Dunod, Paris, 1972.
33. A. Fortin. *Méthodes d'éléments finis pour les équations de Navier–Stokes*. PhD thesis, Université Laval, 1984.

34. A. Fortin and M. Fortin. Newer and newer elements for incompressible flow. In R.H. Gallagher, G.F. Carey, J.T. Oden, and O.C. Zienkiewicz, editors, *Finite Elements in Fluids*, Volume 6. Chichester, England and New York, Wiley-Interscience, 1985, p. 171–187.
35. M. Fortin. Utilisation de la méthode des éléments finis en mécanique des fluides. *Calcolo*, 12:405–441, 1975.
36. M. Fortin. An analysis of the convergence of mixed finite element methods. *R.A.I.R.O. Anal. Numer.*, 11:341–354, 1977.
37. M. Fortin. Old and new finite elements for incompressible flows. *Int. J. Numer. Methods Fluids*, 1:347–364, 1981.
38. M. Fortin, R. Peyret, and R. Temam. Résolution numérique des équations de Navier–Stokes pour un fluide visqueux incompressible. *J. Mécanique*, 10, 3:357–390, 1971.
39. M. Fortin and M. Soulie. A nonconforming piecewise quadratic finite element on triangles. *Int. J. Numer. Methods Eng.*, 19:505–520, 1983.
40. M. Fortin and F. Thomasset. Mixed finite element methods for incompressible flow problems. *J. Comput. Physics*, 37:173–215, 1979.
41. V. Girault and P.A. Raviart. *Finite Element Methods for Navier–Stokes Equations, Theory and Algorithms*. Springer, Berlin Heidelberg New York, 1986.
42. R. Glowinski and O. Pironneau. Numerical methods for the first biharmonic equation and for the two-dimensional Stokes problem. *SIAM Rev.*, 17:167–212, 1979.
43. D. Griffiths. Finite elements for incompressible flow. *Math. Methods Appl. Sci.*, 1:16–31, 1979.
44. F. Hecht. Construction d'une base de fontions P1 non-conformes à divergence nulle dans $\mathbb{R}^3$. *R.A.I.R.O. Anal. Numer.*, 15:119–150, 1981.
45. P. Hood and C. Taylor. Numerical solution of the Navier–Stokes equations using the finite element technique. *Comput. Fluids*, 1:1–28, 1973.
46. T.J.R. Hughes and H. Allik. Finite elements for compressible and incompressible continua. In *Proceedings of the Symposium on Civil Engineering*, Nashville, TN. Vanderbilt University, 1969, pp. 27–62.
47. C. Johnson. On the convergence of a mixed finite element method for plate bending problems. *Numer. Math.*, 21:43–62, 1973.
48. C. Johnson and J. Pitkäranta. Analysis of some mixed finite element methods related to reduced integration. *Math. Comput.*, 38:375–400, 1982.
49. D.S. Malkus. Eigenproblems associated with the discrete LBB-condition for incompressible finite elements. *Int. J. Eng. Sci.*, 19:1299–1310, 1981.
50. D.S Malkus and T.J.R. Hughes. Mixed finite element methods. reduced and selective integration techniques: a unification of concepts. *Comput. Methods Appl. Mech. Eng.*, 15:63–81, 1978.
51. Z. Mghazli. *Une méthode mixte pour les équations de l'hydrodynamique*. PhD thesis, Université de Montréal, 1987.
52. J.T. Oden and O. Jacquotte. Stability of some mixed finite element methods for Stokesian flows. *Comput. Methods Appl. Mech. Eng.*, 43:231–247, 1984.
53. O. Pironneau. *Finite Element Methods for Fluids*. John Wiley, Chichester, 1989. Translated from the French.
54. J. Qin. *On the convergence of some simple finite elements for incompressible flows*. PhD thesis, Penn State University, 1994.
55. R. Rannacher and S. Turek. Simple nonconforming quadrilateral Stokes element. *Numer. Methods Partial Differ. Equations*, 8(2):97–111, 1992.

56. R.L. Sani, P.M. Gresho, R.L. Lee, and D.F. Griffiths. The cause and cure (?) of the spurious pressures generated by certain FEM solutions of the incompressible Navier–Stokes equations. I. *Int. J. Numer. Methods Fluids*, 1(1):17–43, 1981.
57. R. L. Sani, P. M. Gresho, R. L. Lee, D. F. Griffiths, and M. Engelman. The cause and cure (!) of the spurious pressures generated by certain FEM solutions of the incompressible Navier–Stokes equations. II. *Int. J. Numer. Methods Fluids*, 1(2):171–204, 1981.
58. L.R. Scott and M. Vogelius. Norm estimates for a maximal right inverse of the divergence operator in spaces of piecewise polynomials. *Math. Model. Numer. Anal.*, 9:11–43, 1985.
59. R. Stenberg. Analysis of mixed finite element methods for the Stokes problem: a unified approach. *Math. Comput.*, 42:9–23, 1984.
60. R. Stenberg. On the construction of optimal mixed finite element methods for the linear elasticity problem. *Numer. Math.*, 48:447–462, 1986.
61. R. Stenberg. On some three-dimensional finite elements for incompressible media. *Comput. Methods Appl. Mech. Eng.*, 63:261–269, 1987.
62. R. Stenberg. On the postprocessing of mixed equilibrium finite element methods. In W. Hackbusch and K. Witsch, editors, *Numerical Tehchniques in Continuum Mechanics*. Veiweg, Braunschweig, 1987. Proceedings of the Second GAMM-Seminar, Kiel, 1986.
63. R. Stenberg. Error analysis of some finite element methods for the Stokes problem. *Math. Comput.*, 54(190):495–508, 1990. Chesnay, France, 1988.
64. R. Temam. *Navier–Stokes Equations*. North-Holland, Amsterdam, 1977.
65. F. Thomasset. *Implementation of Finite Element Methods for Navier–Stokes Equations*. *Springer Series in Computational Physics*. Springer, Berlin Heidelberg New York, 1981.
66. R. Verfürth. Error estimates for a mixed finite element approximation of the Stokes equation. *R.A.I.R.O. Anal. Numer.*, 18:175–182, 1984.
67. O.C. Zienkiewicz, S. Qu, R.L. Taylor, and S. Nakazawa. The patch text for mixed formulations. *Int. J. Numer. Methods Eng.*, 23:1873–1883, 1986.